

CHALMERS



UNIVERSITY OF GOTHENBURG

*PREPRINT 2011:9*

# Predictions of Catastrophes in Space over Time

ANASTASSIA BAXEVANI  
RICHARD WILSON  
MANUEL SCOTTO

*Department of Mathematical Sciences*

*Division of Mathematical Statistics*

CHALMERS UNIVERSITY OF TECHNOLOGY

UNIVERSITY OF GOTHENBURG

Gothenburg Sweden 2011



Preprint 2011:9

# **Prediction of Catastrophes in Space over Time**

Anastassia Baxevani, Richard Wilson,  
and Manuel Scotto

Department of Mathematical Sciences  
Division of Mathematical Statistics  
Chalmers University of Technology and University of Gothenburg  
SE-412 96 Gothenburg, Sweden  
Gothenburg, May 2011

Preprint 2011:9  
ISSN 1652-9715

---

Matematiska vetenskaper  
Göteborg 2011

# PREDICTION OF CATASTROPHES IN SPACE OVER TIME

ANASTASSIA BAXEVANI, RICHARD WILSON, AND MANUEL SCOTTO

ABSTRACT. Predicting rare events, such as high level up-crossings, for spatio-temporal processes plays an important role in the analysis of the occurrence and impact of potential catastrophes in, for example, environmental settings. Designing a system which predicts these events with high probability, but with few false alarms, is clearly desirable. In this paper an optimal alarm system in space over time is introduced and studied in detail. These results generalize those obtained by de Maré [12] and Lindgren ([17], [18]) for stationary stochastic processes evolving in continuous time and are applied here to stationary Gaussian random fields.

## 1. INTRODUCTION

It is widely believed that the frequency of extreme environmental events, such as heat waves and floods, is increasing due to global warming arising from escalating greenhouse gas concentration and other environmental changes. These events can have potentially catastrophic consequences for human activities, through their impact on health, on natural environments, such as coral reefs, and constructed environments, such as coastal installations and offshore structures. In some situations, such extreme events may occur due to their natural (though rare) occurrence for the process of interest, while in other situations, they may be due to changes in underlying factors, such as a change point or a trend (as is thought with global warming), and hence are becoming more frequent. In either case, the frequency and the impact of extreme events are hard to predict and is of major interest. In this paper, we shall consider the development of models for the detection and warning of the occurrence of future rare events and their magnitudes for the former case, with the potential to be extended to the latter.

---

*Date:* May 11, 2011.

*1991 Mathematics Subject Classification.* 60G10, 60G25, 60G70.

*Key words and phrases.* Gaussian random fields, spatio-temporal models, upcrossings, Palm distribution, alarms, optimal prediction, catastrophes, likelihood ratio, reliability.

There is also a continually increasing capacity to collect data across space and time for many situations, including those in climatology and environmental science, leading to a considerable increase in the amount and complexity of available data. This is driving the development and fitting of complex random spatio-temporal models, based, for instance, on random fields (see, for example, Baxevani et al [5] and [7]). Furthermore, with recent developments in statistical methods for modelling spatial extremes and in multivariate statistical techniques for discrimination, clustering and dimension reduction for spatio-temporal series, and the increasing availability of relevant high-quality data, there is the potential both to deepen understanding of underlying physical phenomena and to aid in the construction of models and tools for forecasting the occurrence and impact of rare events (see, for example, Buishand et al [10], Scotto et al [20], and Friederichs [13]).

The construction of optimal alarm processes to predict potential catastrophes based on level crossings for a random process over time was considered by de Maré [12] and Lindgren ([17], [18]) who described a set of principles for the construction of optimal alarm systems in the continuous time-domain and used it to obtain results for the optimal prediction of level crossings for Gaussian processes. These results were used to develop optimal alarm systems to predict high water levels in the Baltic by Svensson et al [23]. A limitation of the alarm system introduced by Lindgren and de Maré is that it ignores the variation in the model parameters over time. Addressing this issue, Turkman [26] suggested a Bayesian approach with (discrete-time) autoregressive models of order one. Antunes et al [3] extended the results given in [26] to discrete-time autoregressive models of order  $p$  and showed how the alarm characteristics can be numerically obtained. A related problem, which is addressed in this paper, is the development of optimal alarm systems for spatial processes evolving over continuous time.

The possible applications of optimal alarm systems are extensive and include such areas as environmental economics and econometrics. For instance, it is desirable to optimally predict upcrossings of critical levels of random processes giving concentrations of air pollutants, such as ozone, carbon monoxide or sulfur dioxide. Such crossings have implications for, amongst other aspects, public health (for example, see Smith et al [22], Koop and Tole [16] and Tobias and Scotto [25]). In risk management in econometrics, the assessment and forecasting of

market risks or credit risks using probabilistic models is mandatory; for example, forecasting financial risk of lending to customers (Thomas [24]), forecasting the arrival of guests at hotels (Weatherford and Kimes [27]) and forecasting daily stock volatility for option pricing, asset allocation and value-at-risk (Fuentes et al [14]). However, these references do not consider the prediction of future upcrossings or downcrossings. More recently, Costa et al [11] considered optimal alarm systems for financial time series modeled via Fractionally Integrated Asymmetric Power ARCH processes. Further implementation of optimal alarm systems for such situations would be useful.

Potential applications of optimal alarm systems for spatio-temporal settings can be found in short-term forecasting of sea levels; for example, in the planning of offshore operations that have a duration of a few days and on long-term predictions of extreme waves. The latter play a central role for the design of most marine systems, both offshore and coastal, as their design needs to take into account the most severe wave conditions which they need to withstand during their lifetime. Further examples can be found in Niedzielski and Kosek [19], Baxevani and Rychlik [8], and Hopkinson et al [15].

Following a brief review of the principles for the construction of temporal optimal alarm systems introduced by de Maré [12] and Lindgren ([17], [18]), a suitable framework is introduced to transfer their results to spatio-temporal optimal alarm systems in Section 2. Formal definitions of the concepts of catastrophe, alarm systems and optimal alarm regions are also given. Section 3 presents important results which are crucial for deriving the general expressions in Section 4, which is devoted to providing explicit general expressions for the optimal alarm regions and a specific case. In Section 5, an example based on Gaussian random fields exhibiting a Gaussian covariance function is investigated. Finally, some ancillary results related with the theory of multivariate normal densities and matrix theory, useful in proving the main results of the paper and simulating the involved processes, are given in appendices.

## 2. CATASTROPHES AND ALARMS

In this section, the framework and theoretical concepts related to optimal event prediction of level crossings in spatio-temporal processes will be discussed, following the approach taken

by de Maré [12] and Lindgren ([17], [18]), with some modifications and obvious extensions to random fields. Formal definitions of the concepts of catastrophes, alarm systems and optimal alarm regions are given below.

Throughout the following, consider the (potentially catastrophic) spatio-temporal process of interest as a family of spatial random fields indexed by time. Hence, let  $\{\xi(\mathbf{s}, t), \mathbf{s} \in \mathbb{R}^2, t \in \mathbb{R}\}$  denote a zero-mean random field over  $\mathbb{R}^3$ , where  $\mathbf{s}$  usually stands for location in (two-dimensional) space and  $t$  for time. In addition, assume there is a multivariate alarm random field,  $\{\boldsymbol{\eta}(\mathbf{s}, t) = (\eta_1(\mathbf{s}, t), \dots, \eta_k(\mathbf{s}, t)), \mathbf{s} \in \mathbb{R}^2, t \in \mathbb{R}\}$ , for some  $k \in \mathbb{N}$ , and which may, for instance, simply be  $\xi$  and possibly its derivatives. It will be assumed that  $(\xi, \boldsymbol{\eta})$  is (separable) strictly stationary and ergodic over  $t$ , with all components of  $(\xi, \boldsymbol{\eta})$  having finite variances. Assume further that the first order derivatives of all components of  $(\xi, \boldsymbol{\eta})$  with respect to  $t$  exist and are continuous with probability one, and have finite variances. Finally, assume that all joint finite dimensional distributions of  $(\xi, \boldsymbol{\eta})$  and their first order derivatives exist and are non-degenerate. Later, it will be assumed that  $(\xi, \boldsymbol{\eta})$  are Gaussian random fields and conditions will be stated to ensure all first order derivatives exist and are continuous with probability one.

Suppose that there are a number of spatial locations from which  $\boldsymbol{\eta}$  can be observed in order to give an alarm at a number of spatial locations for a catastrophe for the field  $\xi$ ; that is, assume there are two sets of spatial locations:  $(\mathbf{s}_{1j}, j = 1, 2, \dots, n)$  are those at which the alarm process  $\boldsymbol{\eta}$  is observed and  $(\mathbf{s}_{0i}, i = 1, 2, \dots, r)$  are those at which a catastrophe for the random field  $\xi$  is of interest.

The first objective is to choose an alarm process  $\boldsymbol{\eta}$  which predicts  $h$ -time units in advance whether a catastrophe will occur or not. A naive alarm system is obtained by basing  $\boldsymbol{\eta}$  on the predictor random field

$$\hat{\xi}_h(\mathbf{s}, t) = E \left[ \xi(\mathbf{s}, t) \mid \xi(\mathbf{s}_{1j}, t^*), -\infty < t^* \leq t - h; j = 1, 2, \dots, n \right],$$

for  $h > 0$ , and where an alarm is given every time the predictor exceeds a given level for at least one location in some set of given locations  $\mathbf{s}_{0i}, i = 1, 2, \dots, r$ . This alarm system, however, is far from optimal as it does not perform well at detecting level crossings, at locating them accurately in time or in giving as few false alarms as possible. To resolve this

issue for one-dimensional processes, de Maré [12] and Lindgren [18] introduced an optimal alarm system, in the sense that it has a high ability of detecting catastrophes over all alarm systems having the same overall alarm probability. Furthermore, it also predicts the time for an upcrossing better than other possible alarm systems. Their approach is generalised below.

Firstly, what is meant by a catastrophe and an alarm need to be defined. Suppose that a catastrophe is said to be occurring at time  $t$  if  $\boldsymbol{\xi}^r(t) \in C$ , where  $\boldsymbol{\xi}^r(t) = (\xi(\mathbf{s}_{01}, t), \dots, \xi(\mathbf{s}_{0r}, t))$  and  $C \in \mathcal{R}^r$ . Similarly, suppose that an alarm is being given at time  $t$  if  $\boldsymbol{\eta}^m(t) \in A$ , where  $\boldsymbol{\eta}^m(t) = (\boldsymbol{\eta}(\mathbf{s}_{11}, t), \dots, \boldsymbol{\eta}(\mathbf{s}_{1n}, t))$ ,  $A \in \mathcal{R}^m$  (the Borel sets in  $\mathbb{R}^m$ ) and  $m = nk$ . Assume that both  $C$  and  $A$  are such that each is the union of their respective interiors and boundaries, and are connected. Furthermore, it will be assumed that  $\partial C$ , the boundary of  $C$ , is  $(r - 1)$ -dimensional, everywhere continuous and possesses continuous first order derivatives almost everywhere with respect to Lebesgue measure (on  $\mathbb{R}^{r-1}$ ).

The context of interest would usually determine both sets of spatial locations and the choice of  $C$ . As well, it may be that some or all of the locations for the alarm process coincide with those for the catastrophe process. The form of the catastrophe set  $C$  would reflect the occurrence of high levels of the random field  $\xi$  at those locations chosen for  $\xi$ . For example,  $C$  could consist of those points in  $\mathbb{R}^r$  for which at least one of the  $\xi(\mathbf{s}_{0j}, t)$ 's is above some level:

$$(1) \quad C = \{\mathbf{x} \in \mathbb{R}^r : \max(x_1 - u_1, \dots, x_r - u_r) \geq 0\},$$

where  $u_1, \dots, u_r$  are (usually high) levels which may vary according to the spatial location. The choice of  $A$  would reflect information which gives a higher probability of a catastrophe and should be chosen according to some optimality criteria.

The times at which catastrophes and alarms commence is of interest since the optimal alarm region will be derived by conditioning the alarm process  $\boldsymbol{\eta}$  on the event that a catastrophe has commenced at a fixed time. Similarly, the risk of a catastrophe will be defined in terms of the distribution of the catastrophe process  $\xi$  conditioned on the event that the alarm has commenced at a fixed (earlier) time. Hence, the events that  $\boldsymbol{\xi}^r$  enters  $C$  and that  $\boldsymbol{\eta}^m$  enters

$A$  at a fixed time  $t \in \mathbb{R}$  will be denoted by

$$(2) \quad C(t) = \{\xi^r(\cdot) \text{ enters the set } C \text{ at time } t\}$$

and

$$(3) \quad A(t) = \{\eta^m(\cdot) \text{ enters the set } A \text{ at time } t\}.$$

For the following discussion, assume that  $(\xi, \eta)$ ,  $C$  and  $A$  are such that points at which these events occur are isolated in time and that the probabilities of the events  $A(t)$  and  $C(t)$  are zero for a fixed time  $t$  (these will follow from natural assumptions for the random fields and the catastrophe and alarm regions).

As the conditioning events  $C(t)$  and  $A(t)$  have zero probability, it is necessary to indicate how the conditional distributions will be obtained and how they should be interpreted. Under the assumption that  $(\xi, \eta)$  is ergodic and that the point processes over time of entries into  $C$  by  $\xi^r$  and into  $A$  by  $\eta^m$  have finite but non-zero intensities, these probabilities can be defined using Palm distributions. The conditional distributions for  $\xi$  and  $\eta$  thereby obtained can then be interpreted as the distribution for  $\xi$  around points in time at which the alarm process  $\eta^m$  enters the set  $A$  and the distribution for  $\eta$  around points in time at which the catastrophe process  $\xi^r$  enters the set  $C$  respectively. The general results from which the Palm distributions for the conditional processes can be defined are given in Section 3. These will be denoted by  $P^0(\eta \in \cdot | C(t))$  and  $P^0(\xi \in \cdot | A(t))$  respectively, and derived in Section 3.

The probabilities of interest in this setting are: how likely a catastrophe is to occur; how likely an alarm is to occur; how likely a catastrophe is to be occurring at some time given that an alarm commenced at some fixed lag earlier; and how likely an alarm was occurring at some fixed lag earlier given that a catastrophe commenced at some fixed time. Following Lindgren [18], define the following probabilities:

**Definition 1.** *Suppose that  $C \in \mathcal{R}^r$  is a given catastrophe region and  $A \in \mathcal{R}^m$  is a given alarm region.*

(a) *The catastrophe size of  $C$  is given by the probability  $\gamma = P(\xi^r(t) \in C)$ .*

(b) *The alarm size of  $A$  is given by the probability  $\alpha = P(\eta^m(t) \in A)$ .*

(c) *The risk of a catastrophe  $C$  at lag  $h$  for an alarm region  $A$  is given by the probability*

$$\rho_h = P^0(\boldsymbol{\xi}^r(t+h) \in C | A(t)).$$

(d) The detection probability with warning time  $h$  of an alarm  $A$  for a catastrophe  $C$  is given by the probability  $\delta_h = P^0(\boldsymbol{\eta}^m(t) \in A | C(t+h))$ .

It is clear that the catastrophe size  $\gamma$  indicates the proportion of time the catastrophe process is in the catastrophe state, while the alarm size  $\alpha$  indicates the proportion of time the alarm process is in the alarm state. Similarly, the risk  $\rho_h$  indicates the proportion of time the catastrophe process is in the catastrophe state at lag  $h$  after the alarm process entered the alarm state, giving a measure of how accurate the alarm process is. Finally,  $\delta_h$  indicates the proportion of time that the start of a catastrophe had an alarm associated with it exactly  $h$  time units earlier (and hence that the alarm commenced prior to  $h$  time units earlier), giving a measure of how many catastrophes were detected. Note that, as  $(\boldsymbol{\xi}, \boldsymbol{\eta})$  is stationary, the dependence on  $t$  in Definition 1 can be dropped.

Of additional interest are the distributions for the lengths of time for each period of alarm and each period of catastrophe, and the distribution of the time from the start of an alarm till the start of the next catastrophe period, though, of course, there may be a high probability that no catastrophe is associated with a given alarm period. These are not considered here.

As in any diagnostic setting, it is desirable that the detection probability is as close to one as possible while also keeping the risk probability as high as possible (so keeping the number of false alarms low). One way of achieving the first would be to set the alarm region large, but this would clearly decrease the risk probability and lead to a larger number of false alarms. Fixing the size of the alarm region and then choosing the best alarm region in the sense of maximising the detection probability is one way of achieving a compromise.

**Definition 2** (Optimal alarm region). *An alarm region  $A_h$  is said to be optimal for lag  $h$  with associated alarm size  $\alpha_h$ , if it satisfies*

$$(4) \quad P^0(\boldsymbol{\eta}^m(t) \in A_h | C(t+h)) = \sup_B P^0(\boldsymbol{\eta}^m(t) \in B | C(t+h)),$$

where the supremum is taken over all Borel subsets  $B$  in  $\mathbb{R}^m$  such that  $P(\boldsymbol{\eta}^m(t) \in B) \leq \alpha_h$ .

As it is important to consider all lags, an *alarm system* will be defined to be a collection of alarm sizes (which may change with lag) and corresponding alarm regions given over all lags

$h > 0$ :  $\{\alpha_h, A_h; h > 0\}$  with  $\alpha_h = P(\boldsymbol{\eta}^m(t) \in A_h)$ . Definition 2 can then be extended to an alarm system:

**Definition 3** (Optimal alarm system). *An alarm system  $\{\alpha_h, A_h; h > 0\}$  is said to be optimal if each alarm region  $A_h$  is optimal for alarm size  $\alpha_h$  and lag  $h$ .*

The definitions above, however, do not easily translate into clear guidelines on how to choose the *optimal* alarm region  $A_h$  for given lag  $h$  with associated alarm size  $\alpha_h$ . The next result, based on the same principles as those used to obtain “most powerful tests” (see Section 4 of Lindgren [18]), provides an explicit method for deriving the optimal alarm regions:

**Lemma 1** (Optimal alarm regions). *For a given lag  $h$  with associated alarm size  $\alpha_h$ , the alarm region given by*

$$A_h = \left\{ \mathbf{y} \in \mathbb{R}^m : \frac{f_{\boldsymbol{\eta}^m(t)}^0(\mathbf{y} | C(t+h))}{f_{\boldsymbol{\eta}^m(t)}(\mathbf{y})} \geq k_h \right\},$$

*is optimal of size  $\alpha_h$ , where  $f_{\boldsymbol{\eta}^m(t)}^0(\cdot | C(t+h))$  denotes the appropriate density function for the Palm distribution for the conditional process  $\boldsymbol{\eta}^m | C(t+h)$  (that is, the density function for the Palm distribution for  $\boldsymbol{\eta}^m(t)$  given a catastrophe commences at time  $t+h$ ),  $f_{\boldsymbol{\eta}^m(t)}(\cdot)$  is the unconditional multivariate density of the random vector  $\boldsymbol{\eta}^m(t)$  and the nonnegative constants  $k_h$  are such that  $P(\boldsymbol{\eta}^m(t) \in A_h) = \alpha_h$ .*

This result indicates little about the form of the optimal alarm with regard to boundedness, connectivity and so on.

Note: Throughout the paper,  $f(\cdot)$  will denote the probability density function of the subscripted random variable.

### 3. PALM DISTRIBUTIONS AND SLEPIAN MODELS

In order to obtain the results of Sections 4 and 5, the conditional distribution for a multivariate one-dimensional process given a second multivariate one-dimensional process enters a specified region at a given time is required. In this section, this conditional distribution will be derived in terms of Palm distributions. From this, the conditional probability density function and the Slepian model representation for the first process can be obtained. To avoid

introducing new notation, similar notation to that used in earlier sections (and returned to in Section 5) will be modified and used. As the spatial locations considered earlier were fixed, these are incorporated through the multivariate nature of the processes.

Let  $\{(\boldsymbol{\xi}(t), \boldsymbol{\eta}(t)), t \in \mathbb{R}\}$  now denote  $r$ -dimensional and  $m$ -dimensional (separable) strictly stationary and ergodic zero-mean random processes over time respectively, with all components of  $(\boldsymbol{\xi}(t), \boldsymbol{\eta}(t))$  having finite variances. Assume further that the first order derivatives of all components of  $(\boldsymbol{\xi}, \boldsymbol{\eta})$  exist and are continuous with probability one, and have finite variances. Finally, assume that all joint finite dimensional distributions of  $(\boldsymbol{\xi}, \boldsymbol{\eta})$  and their first order derivatives exist and are non-degenerate.

Let  $C$  be some region in  $\mathbb{R}^r$ . Assume that its boundary,  $\partial C$ , is  $(r - 1)$ -dimensional, is everywhere continuous and possesses continuous first order derivatives almost everywhere with respect to Lebesgue measure (on  $\mathbb{R}^{r-1}$ ). Assume further that every point in  $\partial C$  can be obtained as a limit point of an infinite sequence contained in the interior of  $C$ .

To obtain the required results, it is necessary to define the conditional distribution of  $\boldsymbol{\eta}$  given that  $\boldsymbol{\xi}$  enters  $C$  at some fixed time point, which can be taken to be  $t = 0$  without loss of generality since the processes are stationary over time. However, the conditioning event has probability zero and so care needs to be taken in defining the conditional distribution. Since it is assumed that the process is strictly stationary and ergodic, the definition used here will be that given by Palm distributions as this has a natural relative frequency interpretation. Note that, under the assumptions above, the probability is zero that, in a finite interval of time,  $\boldsymbol{\xi}(t)$  takes a value on the boundary of  $C$  at which the first order derivatives do not exist.

The methods required here are very similar to those in Lindgren [17] to obtain the Palm distribution, and subsequently the Slepian model, for the catastrophe process given the alarm process enters the alarm region at a given time point. Consequently, only the key features will be given here. Since entry into the region  $C$  by the process  $\boldsymbol{\xi}$  corresponds to a one dimensional restriction on the process for a fixed time point, the probability that there is an entry into  $C$  by the process  $\boldsymbol{\xi}$  in a non-degenerate interval of time is greater than zero.

To obtain the Palm distribution for  $\boldsymbol{\eta}$  given the event  $C(0)$  occurs, where

$$C(t) = \{\boldsymbol{\xi}(\cdot) \text{ enters } C \text{ through } \partial C \text{ at time } t\},$$

the following point processes need to be defined. Let

$$N_T = \#\{t \in [0, T] : C(t) \text{ occurs}\}$$

and

$$N_T(B_\tau) = \#\{t \in [0, T] : C(t) \text{ occurs and } \boldsymbol{\eta}(t + \cdot) \in B_\tau\}$$

for the number of entries into  $C$  by  $\boldsymbol{\xi}$  through the boundary  $\partial C$  over the interval  $[0, T]$  and the number of such entries for which  $\boldsymbol{\eta}(t + \cdot) \in B_\tau$  respectively, where  $\boldsymbol{\eta}(t + \cdot)$  denotes the process  $\{\boldsymbol{\eta}(t + s), s \in \mathbb{R}\}$  and  $B_\tau$  is a finite dimensional set of the form

$$(5) \quad B_\tau = \{\{\mathbf{y}(t), t \in \mathbb{R}\} : (\mathbf{y}(\tau_1), \dots, \mathbf{y}(\tau_n)) \in B\}$$

for which  $\boldsymbol{\tau} = (\tau_1, \dots, \tau_n) \in \mathbb{R}^n$ ,  $B$  is a Borel set in  $\mathbb{R}^{m \times n}$  and  $n \in \mathbb{N}$ . Assuming the expectations in the following exist (to be shown below), the conditional finite dimensional (Palm) distributions of  $\boldsymbol{\eta}$  given the event  $C(0)$  are defined as

$$(6) \quad P^0 \left( \boldsymbol{\eta}(\boldsymbol{\tau}) \in B_\tau \mid C(0) \right) = \frac{E[N_1(B_\tau)]}{E[N_1]}.$$

Since the finite dimensional distributions are measure determining, these are all that are required in order to define the conditional process.

In order to find the expectations on the right side of (6), it is simplest to use the argument taken by Lindgren [17]. Hence, let  $\mathcal{M}$  be a real valued function satisfying

$$\begin{aligned} \mathbf{x} \in \partial C &\iff \mathcal{M}(\mathbf{x}) = 0 \\ \mathbf{x} \in C &\iff \mathcal{M}(\mathbf{x}) > 0, \end{aligned}$$

and  $\mathcal{M}(\mathbf{x}) < 0$  otherwise, where  $\mathbf{x} = (x_1, \dots, x_r) \in \mathbb{R}^r$ . Since the boundary of  $C$  is smooth almost everywhere, it can be assumed that  $\mathcal{M}(\mathbf{x})$  is continuously differentiable with respect to all components of  $\mathbf{x}$ , at least for  $\mathbf{x}$  near the boundary  $\partial C$  and except possibly for a set of  $((r - 1)$ -dimensional) Lebesgue measure zero on  $\partial C$ . This would be true, for instance, if  $C$  is the region similar to that given by (1).

For each point  $\mathbf{x}$  on the surface determined by  $\mathcal{M}(\mathbf{x}) = c$ , where  $c$  is a fixed constant, and at which  $\mathcal{M}(\mathbf{x})$  is continuously differentiable, denote by  $\boldsymbol{\nu}_{\mathbf{x}}$  the unit vector normal to the surface at the point  $\mathbf{x}$ :

$$\boldsymbol{\nu}_{\mathbf{x}} = \frac{\dot{\mathcal{M}}(\mathbf{x})}{|\dot{\mathcal{M}}(\mathbf{x})|},$$

and for which the gradient  $\dot{\mathcal{M}}(\mathbf{x}) = (\frac{\partial \mathcal{M}}{\partial x_1}, \dots, \frac{\partial \mathcal{M}}{\partial x_r}) \neq \mathbf{0}$ . Thus, for  $\mathbf{x}$  such that  $\mathcal{M}(\mathbf{x}) = 0$ ,  $\boldsymbol{\nu}_{\mathbf{x}}$  is in the direction of increasing values of  $\mathcal{M}$ ; that is, for  $\mathbf{x}$  on the boundary of  $C$ ,  $\boldsymbol{\nu}_{\mathbf{x}}$  is in the direction of entry into  $C$ .

Define a new one-dimensional process by  $\mathcal{M}_t = \mathcal{M}(\boldsymbol{\xi}(t))$ . Since  $\boldsymbol{\xi}$  is stationary and ergodic, it immediately follows that  $\{\mathcal{M}_t, t \in \mathbb{R}\}$  is also stationary and ergodic. In addition to the conditions given above for  $(\boldsymbol{\xi}, \boldsymbol{\eta})$ , assume that, by an appropriate choice of  $\mathcal{M}(\cdot)$ , these processes are such that the conditions of Theorem 11.2.1 of Adler and Taylor [1] are satisfied for  $\{(\mathcal{M}_t, \dot{\mathcal{M}}_t, \boldsymbol{\eta}(t)), t \in \mathbb{R}\}$ , where

$$\dot{\mathcal{M}}_t = \frac{\partial \mathcal{M}(\boldsymbol{\xi}(t))}{\partial t} = \dot{\boldsymbol{\xi}}(t) \cdot \dot{\mathcal{M}}(\boldsymbol{\xi}(t)), \quad \dot{\boldsymbol{\xi}}(t) = \frac{\partial \boldsymbol{\xi}(t)}{\partial t}.$$

These restrictions are not onerous and, for Gaussian processes, are satisfied by the earlier conditions above and appropriate conditions on their covariance functions (such as (11.2.5) on p. 268 of Adler and Taylor [1]). Of course,  $\{\mathcal{M}_t, t \in \mathbb{R}\}$  will not be Gaussian even if  $\boldsymbol{\xi}$  is. However, given the assumptions on  $(\boldsymbol{\xi}, \boldsymbol{\eta})$  and  $\partial C$ , there exists  $\mathcal{M}(\cdot)$  such that these conditions are satisfied.

Hence, since  $\boldsymbol{\xi}(t)$  is a continuously differentiable  $r$ -variate process, the entries into  $C$  through  $\partial C$  by  $\boldsymbol{\xi}(t)$  can be expressed by means of zero-upcrossings by  $\mathcal{M}_t$ . Under the above assumptions on  $\boldsymbol{\xi}$  and  $C$ , these points are isolated, lie on  $\partial C$  and are points at which  $\{\mathcal{M}_t, t \in \mathbb{R}\}$  is continuously differentiable with probability one. Thus, the event that  $\boldsymbol{\xi}(\cdot)$  enters  $C$  at time  $t$  is given by

$$C(t) = \{\mathcal{M}_t = 0, \dot{\mathcal{M}}_t > 0\}.$$

If  $\gamma_{\boldsymbol{\xi}}$  denotes the intensity of such entries through  $\partial C$ , then it is simply the expected number of zero up-crossings in  $[0, 1]$  for  $\mathcal{M}$ . Hence, similarly to Theorem 4.2 of Lindgren [17], it is given by Rice's formula (see Theorem 11.2.1 of Adler and Taylor [1]):

**Theorem 1.** *The mean number of entries into  $C$  from  $C^c$  across the boundary  $\partial C$  per time unit is given by:*

$$\begin{aligned}
\gamma_{\xi} &= E(N_1) = f_{\mathcal{M}_0}(0)E \left[ (\dot{\mathcal{M}}_0)^+ \mid \mathcal{M}_0 = 0 \right] \\
&= \int_{z=0}^{\infty} z f_{\mathcal{M}_0, \dot{\mathcal{M}}_0}(0, z) dz \\
(7) \quad &= \int_{\mathbf{x} \in \partial C} q(\mathbf{x}) f_{\xi(0)}(\mathbf{x}) ds(\mathbf{x})
\end{aligned}$$

where

$$q(\mathbf{x}) = |\dot{\mathcal{M}}(\mathbf{x})|^{-1} E \left[ [(\dot{\mathcal{M}}_0)^+ \mid \xi(0) = \mathbf{x}] \right] = E \left[ (\boldsymbol{\nu}_{\mathbf{x}} \cdot \dot{\xi}(0))^+ \mid \xi(0) = \mathbf{x} \right]$$

and  $ds(\mathbf{x})$  is the surface element on  $\partial C$ .

Note that  $\partial C$  may include regions on which  $\mathcal{M}(\cdot)$  is not differentiable. However, these are of Lebesgue measure 0 and are hence of no concern. Strictly speaking, the integral in (7) above should be written as a (possibly countably infinite) sum of integrals over the disjoint regions of  $\partial C$  for which  $\mathcal{M}(\cdot)$  is differentiable in order to exclude those regions on which  $\mathcal{M}(\cdot)$  is not differentiable. For ease of notation and explanation, this will not be done.

Hence, from the ergodic theorem and in a similar fashion to Theorem 4.4 of Lindgren [17], the conditional finite dimensional distributions for  $\boldsymbol{\eta}$  given  $C(0)$  defined by (6) can be obtained in terms of the random process  $\mathcal{M}_t = \mathcal{M}(\xi(t))$  (again, the expressions for the expected values follow immediately from Theorem 11.2.1 of Adler and Taylor [1]):

**Theorem 2.** *Under the above assumptions on  $(\xi, \boldsymbol{\eta})$ ,  $C$  and  $\mathcal{M}$ , it follows that, with probability one,*

$$\begin{aligned}
\lim_{T \rightarrow \infty} \frac{N_T(B_{\tau})}{N_T} &= \frac{E[N_1(B_{\tau})]}{E[N_1]} \\
&= \frac{f_{\mathcal{M}_0}(0)E \left[ I\{\boldsymbol{\eta}(0 + \cdot) \in B_{\tau}\} (\dot{\mathcal{M}}_0)^+ \mid \mathcal{M}_0 = 0 \right]}{f_{\mathcal{M}_0}(0)E \left( (\dot{\mathcal{M}}_0)^+ \mid \mathcal{M}_0 = 0 \right)} \\
&= \frac{1}{\gamma_{\xi}} \int_{z=0}^{\infty} z P \left( \boldsymbol{\eta}(0 + \cdot) \in B_{\tau} \mid \mathcal{M}_0 = 0, \dot{\mathcal{M}}_0 = z \right) f_{\mathcal{M}_0, \dot{\mathcal{M}}_0}(0, z) dz \\
&= \frac{1}{\gamma_{\xi}} \int_{z=0}^{\infty} \int_{\mathbf{y} \in B} z f_{\mathcal{M}_0, \dot{\mathcal{M}}_0, \boldsymbol{\eta}_{\tau}(0)}(0, z, \mathbf{y}) dz d\mathbf{y}.
\end{aligned}$$

where

$$\boldsymbol{\eta}_\tau = (\boldsymbol{\eta}(\tau_1), \dots, \boldsymbol{\eta}(\tau_n))$$

and  $B_\tau$ ,  $(\tau_1, \dots, \tau_n)$ ,  $B$  and  $n$  are as in (5). Here,  $I\{\cdot\}$  denotes the indicator function of the contained event (and equals one when the contained event occurs and is zero otherwise).

Following Lindgren [17], the above integrals, which involve the joint density of  $(\mathcal{M}_0, \dot{\mathcal{M}}_0)$  and the conditional density of  $\boldsymbol{\eta}_\tau(0)$  given  $\{\mathcal{M}_0 = 0, \dot{\mathcal{M}}_0 = z\}$  (which usually do not have simple closed forms), can be written as surface integrals in terms of the distribution of  $\boldsymbol{\xi}$  and its derivative:

**Theorem 3.** *Under the above assumptions on  $(\boldsymbol{\xi}, \boldsymbol{\eta})$  and  $C$ , and assuming  $B_\tau$  given by (5) is open, then*

$$\begin{aligned} \frac{E[N_1(B_\tau)]}{E[N_1]} &= \frac{1}{\gamma_\xi} \int_{\mathbf{x} \in \partial C} \int_{\mathbf{z} \in \mathbb{R}^r} (\boldsymbol{\nu}_\mathbf{x} \cdot \dot{\boldsymbol{\xi}}(0))^+ P(\boldsymbol{\eta}(0) \in B_\tau | \boldsymbol{\xi}(0) = \mathbf{x}, \dot{\boldsymbol{\xi}}(0) = \mathbf{z}) \\ &\quad \times f_{\boldsymbol{\xi}(0), \dot{\boldsymbol{\xi}}(0)}(\mathbf{x}, \mathbf{z}) d\mathbf{z} ds(\mathbf{x}), \\ (8) \quad &= \frac{1}{\gamma_\xi} \int_{\mathbf{x} \in \partial C} \int_{\mathbf{z} \in \mathbb{R}^r} \int_{\mathbf{y} \in B} (\boldsymbol{\nu}_\mathbf{x} \cdot \mathbf{z})^+ f_{\boldsymbol{\xi}(0), \dot{\boldsymbol{\xi}}(0), \boldsymbol{\eta}_\tau(0)}(\mathbf{x}, \mathbf{z}, \mathbf{y}) d\mathbf{y} d\mathbf{z} ds(\mathbf{x}), \end{aligned}$$

where  $ds(\mathbf{x})$  is the surface element on  $\partial C$  (see previous note).

In order to obtain the optimal alarm region, the probability density function of the conditional process is required. This is obtained simply from the above result:

**Corollary 1.** *The conditional probability density function for the process at  $(\tau_1, \dots, \tau_n)$  is*

$$(9) \quad \frac{1}{\gamma_\xi} \int_{\mathbf{x} \in \partial C} \int_{\mathbf{z} \in \mathbb{R}^r} (\boldsymbol{\nu}_\mathbf{x} \cdot \mathbf{z})^+ f_{\boldsymbol{\xi}(0), \dot{\boldsymbol{\xi}}(0), \boldsymbol{\eta}_\tau(0)}(\mathbf{x}, \mathbf{z}, \mathbf{y}) d\mathbf{z} ds(\mathbf{x}).$$

An immediate consequence of Theorem 3 is the joint long-run distribution of the process  $\boldsymbol{\xi}$  and its derivative at its entries into  $C$ . To obtain this result, simply take  $\boldsymbol{\eta}$  as  $(\boldsymbol{\xi}, \dot{\boldsymbol{\xi}})$  with  $n = 1$  and  $\tau_1 = 0$  in Theorem 3:

**Corollary 2.** *Let  $\{\hat{t}_j, j \in \mathbb{Z}\}$  denote the times at which  $\boldsymbol{\xi}(\cdot)$  enters  $C$ . Under the above assumptions on  $\boldsymbol{\xi}$  and  $C$ , the long-run joint distribution of the height  $\boldsymbol{\xi}(\hat{t}_j)$  and the directional derivative  $\dot{\boldsymbol{\xi}}(\hat{t}_j)$  at the entries of  $\boldsymbol{\xi}(\cdot)$  across the boundary  $\partial C$  into  $C$  is given by*

$$\frac{(\boldsymbol{\nu}_\mathbf{x} \cdot \mathbf{z})^+}{\gamma_\xi} f_{\boldsymbol{\xi}(0), \dot{\boldsymbol{\xi}}(0)}(\mathbf{x}, \mathbf{z}) d\mathbf{z} ds(\mathbf{x}).$$

This follows from the fact that  $q(\cdot, \mathbf{x})$  is absolutely continuous with respect to  $p(\cdot, \mathbf{x})$  with density

$$\frac{dq(\cdot, \mathbf{x})}{dp(\cdot, \mathbf{x})} = (\boldsymbol{\nu}_{\mathbf{x}} \cdot \mathbf{z})^+,$$

where

$$q(B, \mathbf{x}) = E \left[ I\{\dot{\boldsymbol{\xi}}(0) \in B\} \left( \boldsymbol{\nu}_{\mathbf{x}} \cdot (\dot{\boldsymbol{\xi}}(0)) \right)^+ \mid \boldsymbol{\xi}(0) = \mathbf{x} \right],$$

for  $B$  a Borel set in  $\mathbb{R}^r$ , and  $dp(\cdot, \mathbf{x}) = f_{\dot{\boldsymbol{\xi}}(0) \mid \boldsymbol{\xi}(0)=\mathbf{x}}(\cdot)$ .

From this point on, assume that  $(\boldsymbol{\xi}, \boldsymbol{\eta})$  are jointly Gaussian and that the covariance functions of the components of  $\boldsymbol{\xi}$ ,  $\dot{\boldsymbol{\xi}}$  and  $\boldsymbol{\eta}$  satisfy condition (11.2.5) on p.268 of Adler and Taylor [1]. To obtain the multivariate version of the long-run Rayleigh distribution of the derivative of a Gaussian process at an upcrossing (classical theory), the following results are needed from the theory of multivariate normal random variables.

**Lemma 2.** *Under the above assumptions on  $(\boldsymbol{\xi}, \boldsymbol{\eta})$ , the conditional distribution of*

$$\boldsymbol{\eta}(t) \mid \left( \boldsymbol{\xi}(0) = \mathbf{x}, \dot{\boldsymbol{\xi}}(0) = \mathbf{z} \right)$$

*is  $m$ -variate normal with mean vector*

$$(10) \quad \mathbf{m}_{\mathbf{x}, \mathbf{z}}^{\boldsymbol{\eta}}(t) = [r_{\boldsymbol{\xi}, \boldsymbol{\eta}}(t)^T \quad -\dot{r}_{\boldsymbol{\xi}, \boldsymbol{\eta}}(t)^T] r_{\boldsymbol{\xi}, \dot{\boldsymbol{\xi}}}(0)^{-1} \begin{bmatrix} \mathbf{x} \\ \mathbf{z} \end{bmatrix}$$

*and covariance matrix function*

$$(11) \quad \begin{aligned} r_{\mathbf{x}, \mathbf{z}}^{\boldsymbol{\eta}}(t_1, t_2) &= \text{Cov}(\boldsymbol{\eta}(t_1), \boldsymbol{\eta}(t_2) \mid \boldsymbol{\xi}(0) = \mathbf{x}, \dot{\boldsymbol{\xi}}(0) = \mathbf{z}) \\ &= r_{\boldsymbol{\eta}}(t_1 - t_2) - [r_{\boldsymbol{\xi}, \boldsymbol{\eta}}(t_1)^T \quad -\dot{r}_{\boldsymbol{\xi}, \boldsymbol{\eta}}(t_1)^T] r_{\boldsymbol{\xi}, \dot{\boldsymbol{\xi}}}(0)^{-1} \begin{bmatrix} r_{\boldsymbol{\xi}, \boldsymbol{\eta}}(t_2) \\ -\dot{r}_{\boldsymbol{\xi}, \boldsymbol{\eta}}(t_2) \end{bmatrix}, \end{aligned}$$

where  $r_{\boldsymbol{\xi}, \dot{\boldsymbol{\xi}}}(0)$  is the covariance matrix of  $(\boldsymbol{\xi}(t), \dot{\boldsymbol{\xi}}(t))$ ,  $r_{\boldsymbol{\eta}}(t_1 - t_2)$  is the covariance matrix function of  $\boldsymbol{\eta}$  and  $r_{\boldsymbol{\xi}, \boldsymbol{\eta}}(t)$  is the cross covariance matrix of  $\boldsymbol{\xi}$  and  $\boldsymbol{\eta}$ , and are matrices of dimensions  $2r \times 2r$ ,  $m \times m$  and  $m \times r$  respectively. As (11) does not depend on either  $\mathbf{x}$  or  $\mathbf{z}$ , it will written as  $r^{\boldsymbol{\eta}}(t_1, t_2) = r_{\mathbf{x}, \mathbf{z}}^{\boldsymbol{\eta}}(t_1, t_2)$ .

The Slepian model representation for the conditional process  $\boldsymbol{\eta} \mid C(0)$  can now be stated. Firstly, let  $\boldsymbol{\kappa}(t)$  denote a non-stationary  $m$ -dimensional normal process with mean zero and

the covariance matrix  $r^\eta(t_1, t_2)$  given in (11). Additionally, let  $(\boldsymbol{\chi}, \boldsymbol{\zeta})$  be a  $2r$ -dimensional random variable independent of  $\boldsymbol{\kappa}$ , taking values on

$$\{(\mathbf{x}, \mathbf{z}) \in \partial C^- \times \mathbb{R}^r : \boldsymbol{\nu}_\mathbf{x} \cdot \mathbf{z} > 0 \text{ for each } \mathbf{x} \in \partial C^-\}$$

and with distribution given by

$$f_{\boldsymbol{\chi}, \boldsymbol{\zeta}}(\mathbf{x}, d\mathbf{z}) ds(\mathbf{x}) = \frac{\boldsymbol{\nu}_\mathbf{x} \cdot \mathbf{z}}{\gamma_\xi} f_{\xi(0)|\xi(0)}(\mathbf{z}|\mathbf{x}) f_{\xi(0)}(\mathbf{x}) d\mathbf{z} ds(\mathbf{x}),$$

where  $\partial C^-$  denotes all those points in  $\partial C$  at which  $\partial C$  possesses all first order derivatives. Define the process  $\{\boldsymbol{\eta}_{\partial C}^m(t), t \in \mathbb{R}\}$  by

$$\boldsymbol{\eta}_{\partial C}(t) = \mathbf{m}_{\boldsymbol{\chi}, \boldsymbol{\zeta}}^\eta(t) + \boldsymbol{\kappa}(t)$$

where  $\mathbf{m}_{\boldsymbol{\chi}, \boldsymbol{\zeta}}^\eta(t)$  is defined in (10).

The following theorem can be obtained using the characteristic functions for the finite dimensional distributions given by (8) and those for  $\boldsymbol{\eta}_{\partial C}$ :

**Theorem 4.** *Under the conditions on  $(\boldsymbol{\xi}, \boldsymbol{\eta})$  and  $C$  (and its boundary) given in this section, the finite dimensional distributions given by (6) for the conditional process  $\boldsymbol{\eta}|C(0)$  are the same as those for the process  $\boldsymbol{\eta}_{\partial C}$ .*

Under ergodicity, Theorem 3 motivates the use of the process  $\boldsymbol{\eta}_{\partial C}$  as a model vector process for  $\boldsymbol{\eta}$  “around” entries of  $\boldsymbol{\xi}$  into  $C$ . It can be used to obtain model vector processes for the alarm process around entries of the catastrophe process into the catastrophe region and for the catastrophe process around entries of the alarm process into the alarm region. These model vector processes can then be used to calculate the different probabilities in definition 1.

#### 4. OPTIMAL ALARMS AND SLEPIAN MODELS

The results of Section 3 will be used in this section to obtain the densities required to determine the optimal alarm regions given in Lemma 1 for both a general setting and a specific case. Assume that the notation for the catastrophe and alarm processes of Section 2 again applies. The results of Section 3 can also be used to obtain Slepian model representations for the conditional (or Palm) processes  $\boldsymbol{\eta}|C(0)$  and  $\xi|A_{opt}(0)$ , where  $A_{opt}$  denotes the optimal

alarm region. The Slepian model representations can be used to obtain the probabilities given by (c) and (d) in Definition 1.

Assume that, in addition to being stationary and ergodic over  $t$ ,  $(\xi, \boldsymbol{\eta})$  is a multi-variate Gaussian random field for which all associated covariance matrices are non-degenerate and all associated covariance functions are twice differentiable and continuous with respect to  $t$ . Suppose as well that

$$(12) \quad \max_r |r(\mathbf{s}_1, \mathbf{s}_2, 0) - r(\mathbf{s}_1, \mathbf{s}_2, t)| \leq K |\ln |t||^{-(1+\alpha)}$$

for some finite  $K > 0$ ,  $\alpha > 0$  and  $t$  small enough, and where  $r$  runs over the second order derivatives with respect to  $t$  of all covariance and cross-covariance functions of  $(\xi, \boldsymbol{\eta})$ . It follows from Corollary 11.2.2 of Adler and Taylor [1] that the conditions of Theorem 11.2.1 of Adler and Taylor [1] hold. Hence, the finite dimensional distributions of the conditional random fields  $\boldsymbol{\eta} | C(0)$  and  $\xi | A(0)$  in the sense of Palm distributions are given by Theorem 3 with the appropriate changes in notation provided  $C$  and  $A$  satisfy the conditions given in Section 2. Note that it has not been assumed that  $(\xi, \boldsymbol{\eta})$  are stationary and ergodic in  $\mathbf{s}$ , and that the Gaussian assumption can be dropped, but then condition (12) becomes much less succinct!

It follows that the (Palm) probability density function for  $\boldsymbol{\eta}^m | C(0)$ , where the event  $C(0)$  is given by (2) for  $C$  satisfying the conditions given in Section 2, is given by Corollary 1. Hence, taking into account that  $(\xi, \boldsymbol{\eta})$  is stationary over time so the dependence on  $t$  in Lemma 1 can be dropped, the optimal alarm region is as follows:

**Theorem 5.** *For a given lag  $h$  with associated alarm size  $\alpha_h$ , the alarm region given by*

$$(13) \quad A_h = \left\{ \mathbf{y} \in \mathbb{R}^m : \int_{\mathbf{x} \in \partial C} \int_{\mathbf{z} \in \mathbb{R}^r} (\boldsymbol{\nu}_{\mathbf{x}} \cdot \mathbf{z})^+ f_{\boldsymbol{\xi}^r(h), \dot{\boldsymbol{\xi}}^r(h)} | \boldsymbol{\eta}^m(0) (\mathbf{x}, \mathbf{z} | \mathbf{y}) d\mathbf{z} ds(\mathbf{x}) \geq k_h \right\},$$

*is optimal of size  $\alpha_h$ , where  $\dot{\boldsymbol{\xi}}^r$  denotes the derivative of  $\boldsymbol{\xi}^r$  with respect to  $t$ ,  $\boldsymbol{\nu}_{\mathbf{x}}$  is the unit vector normal to the surface  $\partial C$  at the point  $\mathbf{x}$  in the direction of entry into  $C$  and the nonnegative constants  $k_h$  are such that  $P(\boldsymbol{\eta}^m(t) \in A_h) = \alpha_h$ .*

The integral in (13) with respect to  $\mathbf{x}$  should really be written as a sum of integrals over those regions for which  $\partial C$  is smooth (see cases below and note after Theorem 1), where  $ds(\mathbf{x})$  is the surface element on  $\partial C$ .

The region given by (13) is difficult to interpret for the general case, so for the remainder of this section it will be assumed that  $C$  takes the form given by (1). Thus,

$$\partial C = \{\mathbf{x} \in \mathbb{R}^r; \max_i x_i = u_i\} = \cup_{i=1}^r \partial C_i$$

where  $\partial C_i = \{\mathbf{x} \in \mathbb{R}^n; x_i = u_i, x_j \leq u_j, j \neq i\}$  for  $i = 1, 2, \dots, r$ , and the integral with respect to  $\mathbf{x}$  can be written as a sum of integrals over the  $\partial C_i$ 's. As well, the unit vector normal to  $\partial C_i$  at  $\mathbf{x}$  in the direction of entry into  $C$  is then simply the  $i^{\text{th}}$  unit vector  $\boldsymbol{\nu}_{\mathbf{x}} = \delta_i = (0, \dots, 1, \dots, 0)$  for all  $\mathbf{x} \in \partial C_i$ ; that is, a zero vector with a one in the  $i^{\text{th}}$  position. Hence, the optimal alarm region can be written as follows:

**Corollary 3.** *For a given lag  $h$  with associated alarm size  $\alpha_h$ , the alarm region given by*

$$\begin{aligned} A_h &= \left\{ \mathbf{y} \in \mathbb{R}^m : \sum_{i=1}^r \int_{\mathbf{x} \in \partial C_i} \int_{\{\mathbf{z} \in \mathbb{R}^r; z_i > 0\}} z_i f_{\boldsymbol{\xi}^r(h), \dot{\boldsymbol{\xi}}^r(h) | \boldsymbol{\eta}^m(0)}(\mathbf{x}, \mathbf{z} | \mathbf{y}) d\mathbf{z} d\mathbf{x}^i \geq k_h \right\} \\ &= \left\{ \mathbf{y} \in \mathbb{R}^m : \sum_{i=1}^r \left( \prod_{j \neq i} \int_{-\infty}^{u_j} \right) \left[ \int_0^\infty z_i f_{\dot{\xi}_i(h) | \boldsymbol{\xi}^r(h), \boldsymbol{\eta}^m(0)}(z_i | \mathbf{x}_u^i, \mathbf{y}) dz_i \right] \right. \\ &\quad \left. \times f_{\boldsymbol{\xi}^r(h) | \boldsymbol{\eta}^m(0)}(\mathbf{x}_u^i | \mathbf{y}) d\mathbf{x}^i \geq k_h \right\}, \\ (14) \quad &= \left\{ \mathbf{y} \in \mathbb{R}^m : \sum_{i=1}^r \left( \prod_{j \neq i} \int_{-\infty}^{u_j} \right) \left[ \dot{\sigma}_i(h) \Psi \left( \frac{\dot{\mu}_i(\mathbf{x}_u^i, \mathbf{y}; h)}{\dot{\sigma}_i(h)} \right) \right] f_{\boldsymbol{\xi}^r(h) | \boldsymbol{\eta}^m(0)}(\mathbf{x}_u^i | \mathbf{y}) d\mathbf{x}^i \geq k_h \right\}, \end{aligned}$$

is optimal of size  $\alpha_h$ , where  $\mathbf{x}_u^i = (x_1, \dots, x_{i-1}, u_i, x_{i+1}, \dots, x_r)$ ,  $d\mathbf{x}^i = dx_1 \dots dx_{i-1} dx_{i+1} \dots dx_r$ ,

$$(15) \quad \dot{\mu}_i(\mathbf{x}_u^i, \mathbf{y}; h) = \mu_{\dot{\xi}_i(h) | \boldsymbol{\xi}^r(h), \boldsymbol{\eta}^m(0)}(\mathbf{x}_u^i, \mathbf{y}; h) \quad \text{and} \quad \dot{\sigma}_i^2(h) = \sigma_{\dot{\xi}_i(h) | \boldsymbol{\xi}^r(h), \boldsymbol{\eta}^m(0)}^2(h)$$

are the conditional mean and variance respectively of  $\dot{\xi}_i(h)$  given  $\boldsymbol{\xi}^r(h) = \mathbf{x}_u^i$  and  $\boldsymbol{\eta}^m(0) = \mathbf{y}$ ,

$$(16) \quad \Psi(z) = \phi(z) + z\Phi(z),$$

with  $\phi(z)$  and  $\Phi(z)$  the standard normal probability density function and distribution function respectively, and the nonnegative constants  $k_h$  are such that  $P(\boldsymbol{\eta}^m(t) \in A_h) = \alpha_h$ . Here, (16) arises from  $\int_0^\infty x f_X(x) dx = \sigma \Psi(\mu/\sigma)$  for  $X \sim N(\mu, \sigma^2)$ .

The conditional mean and variance given by (15) can be obtained using multi-variate normal theory (see Lemma 3 and the cases in the next section), with the mean but not the variance depending on the values of the conditioning variables. The integrals in (14) are non-trivial to

evaluate and so will only be done here numerically for the examples in the following section. Note that the results of Lindgren [18] are a special case of the above result, with  $r = 1$  (see Cases 1 and 2 below), so that the optimal alarm region is then just

$$(17) \quad A_h = \left\{ \mathbf{y} \in \mathbb{R}^m : \dot{\sigma}(h) \Psi \left( \frac{\dot{\mu}(u, \mathbf{y}; h)}{\dot{\sigma}(h)} \right) f_{\xi(h)|\boldsymbol{\eta}^m(0)}(u|\mathbf{y}) \geq k_h \right\},$$

where  $u = u_1$ ,  $\xi(t) = \xi(\mathbf{s}_{01}, t)$  and  $\dot{\mu}$  and  $\dot{\sigma}$  are defined similarly as in (15).

To illustrate the form of the optimal alarm region, four simple cases will be considered and discussed. (To simplify further, it will be assumed that the catastrophe and alarm fields are the same (so  $k = 1$ ).) The cases considered are for when there are (1) single locations for both the catastrophe and alarm processes, (2) a single location for the catastrophe process and two locations for the alarm process, (3) two locations for the catastrophe process and a single location for the alarm process and (4) two locations for both the catastrophe and alarm processes. All locations in space will be assumed to be distinct.

## 5. SPECIAL CASES

The special cases described at the end of the previous section are used in this section to illustrate both the characteristic features of the optimal alarm regions and the related probabilities through a simulation study. For simplicity, it is assumed that the alarm and catastrophe random fields are the same random field (though observed at distinct locations). It is also assumed that this random field is stationary Gaussian with zero mean and covariance function given by

$$(18) \quad r(x, y, t) = \lambda_0 \exp \left( -\frac{1}{2\lambda_0} (x, y, t) \Lambda (x, y, t)' \right),$$

(a Gaussian covariance function) with

$$\Lambda = \begin{pmatrix} \lambda_{200} & \lambda_{110} & \lambda_{101} \\ \lambda_{110} & \lambda_{020} & \lambda_{011} \\ \lambda_{101} & \lambda_{011} & \lambda_{002} \end{pmatrix}$$

where  $\lambda_0 > 0$  is the variance of the random field and  $\Lambda$ , the matrix of second order spectral moments, is positive definite. Amongst other applications, this covariance function has been used to model the spatio-temporal variability of significant wave height (see Baxevani *et al*

[7] and [6]). For the simulations (see Appendix 2 for the simulation procedure), it will be assumed that the variance is one ( $\lambda_0 = 1$ ) and that

$$\Lambda = \begin{pmatrix} 0.9 & 0.3 & 0.09 \\ 0.3 & 0.5 & -0.3 \\ 0.09 & -0.3 & 0.8 \end{pmatrix}.$$

**Case (1)** In the first case, single spatial locations are considered for both the alarm and catastrophe processes. Without loss of generality, the location considered for the catastrophe process will be assumed to be at  $\mathbf{s}_{01} = \mathbf{0}$  and it will be assumed that a catastrophe is occurring at time  $t$  if the level  $u = 2$  is exceeded:  $\xi(\mathbf{0}, t) \geq 2$ . Hence, a catastrophe starts with an upcrossing of the level  $u = 2$ . In order to compare different scenarios for a single time lag  $h$ , four different locations will be considered for the alarm process. As the optimal alarm region is dependent on the interplay (measured through the covariance) between the catastrophe process and the alarm process and between the (time) derivative of the catastrophe process and the alarm process at the chosen time lag, these were chosen on the basis of different combinations of covariances as in the following table:

Alarm Location: $\mathbf{s}_{11}$	$Cov(\xi(\mathbf{0}, h), \eta(\mathbf{s}_{11}, 0))$ ,	$Cov(\dot{\xi}(\mathbf{0}, h), \eta(\mathbf{s}_{11}, 0))$
(-1,2)	0.4274	-0.2949
(-0.4,1)	0.8171	-0.2745
(0.2,-0.4)	0.9666	0.1334
(2.25,-3)	0.0818	0.0902

TABLE 1

To illustrate the form of these pairs of covariances for different lags, the covariance functions  $Cov(\xi(\mathbf{0}, t), \eta(\mathbf{s}_{11}, 0))$  and  $Cov(\dot{\xi}(\mathbf{0}, t), \eta(\mathbf{s}_{11}, 0))$  have been plotted in Figure 1 (top and bottom respectively) for  $\mathbf{s}_{11} = (-1, 2)$ , where the other combinations of locations are similar. Note that, in all cases, the greatest correlation between  $\xi(\mathbf{s}_{01}, t)$  and  $\eta(\mathbf{s}_{11}, 0)$  is at the same lag as when  $\dot{\xi}(\mathbf{s}_{01}, t)$  and  $\eta(\mathbf{s}_{11}, 0)$  are uncorrelated.

For each of the chosen combinations of locations and for the catastrophe as given above, the optimal alarm regions of nominal size  $\alpha = 0.05$  were determined using (14) to obtain alarm

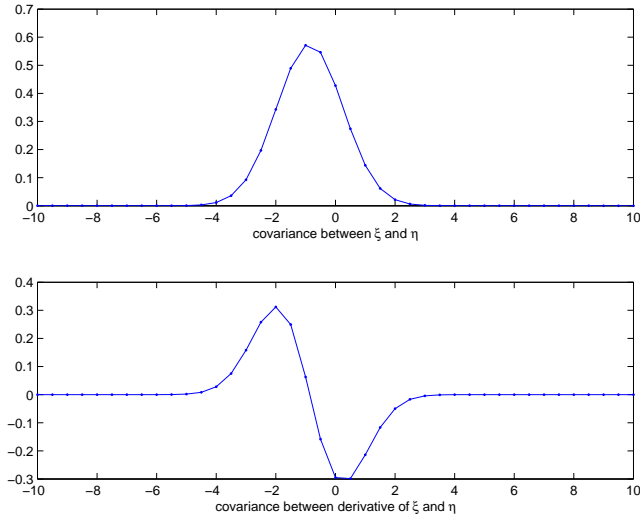


FIGURE 1. Covariance functions between  $\xi(\mathbf{0}, t)$  and  $\eta((-1, 2), 0)$  (*top*) and between  $\dot{\xi}(\mathbf{0}, t)$  and  $\eta((-1, 2), 0)$  (*bottom*).

regions and their corresponding alarm size. The optimal alarm region was then taken to be the region for which  $\alpha \in [0.045, 0.055]$  was closest to 0.05. The regions have been plotted in Figure 2 against their spatial location. For this case, the alarm region takes the form of a bounded interval since the catastrophe starts with an upcrossing and hence the alarm process cannot be “too high” for a close earlier time. Consequently, by considering Table 1, it can be seen that the greater the correlation between the catastrophe process and the alarm process, the smaller the alarm region (as might be expected). The correlation between the derivative of the catastrophe process and the alarm process seems to play a lesser role.

The risk and detection probabilities for a catastrophe occurring at  $\mathbf{s}_{01} = \mathbf{0}$ , an alarm located at  $\mathbf{s}_{11} = (-1, 2)$  and with alarm size  $\alpha \in [0.045, 0.055]$  have been computed using 10 day simulations of the alarm and catastrophe processes. These have been plotted in Figure 3 (top and bottom respectively) for warning times between 0 and 5, and time step of 0.25.

To illustrate the interplay between the alarm and catastrophe processes, simulations for the alarm location  $\mathbf{s}_{11} = (-1, 2)$  were obtained using the procedure outlined in Appendix 2: see top two graphs in Figure 4. The red sections highlight the times when a catastrophe is occurring (the times the catastrophe process exceeds level  $u = 2$ ), while the green sections indicate the alarm times for a possible catastrophe  $h = 0.5$  time units later, where the optimal alarm region was obtained for an alarm size of  $\alpha \in [0.045, 0.055]$ . In Figure 4 (Bottom), the

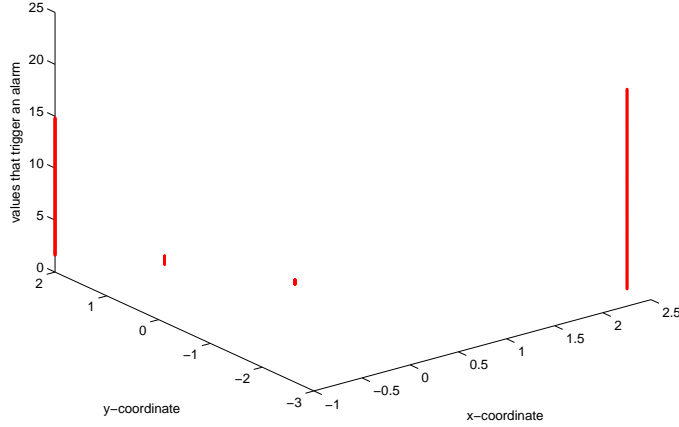


FIGURE 2. Optimal alarm regions for each of the four alarm locations with catastrophe location at  $\mathbf{s}_{01} = \mathbf{0}$ .

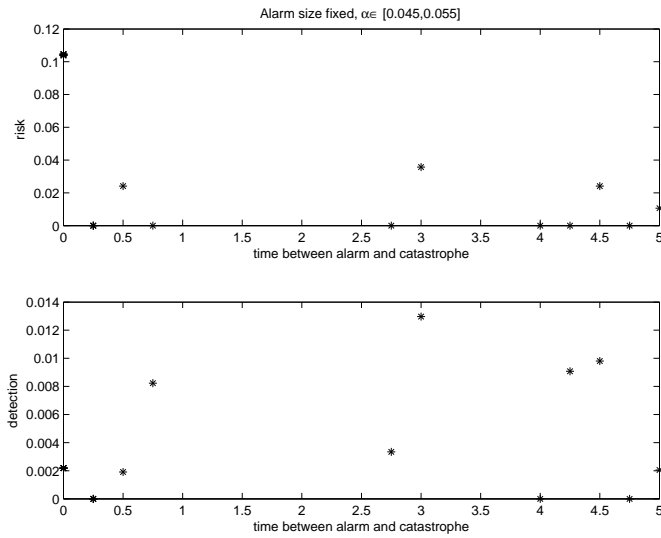


FIGURE 3. Risk probability (*top*) and detection probability (*bottom*) by warning times for catastrophe location  $\mathbf{s}_{01} = \mathbf{0}$ , alarm location  $\mathbf{s}_{11} = (-1, 2)$  and alarm size  $\alpha \in [0.045, 0.055]$ .

same information is indicated without the sample paths so that the relationship can be seen more clearly.

**Case (2)** In this case, there are two locations at which an alarm may be given for a catastrophe at a single location. The same location for a catastrophe as in Case (1) is used here ( $\mathbf{s}_{01} = \mathbf{0}$ ), with the same definition of a catastrophe ( $\xi(\mathbf{0}, t) \geq 2$ ). Each one of the locations

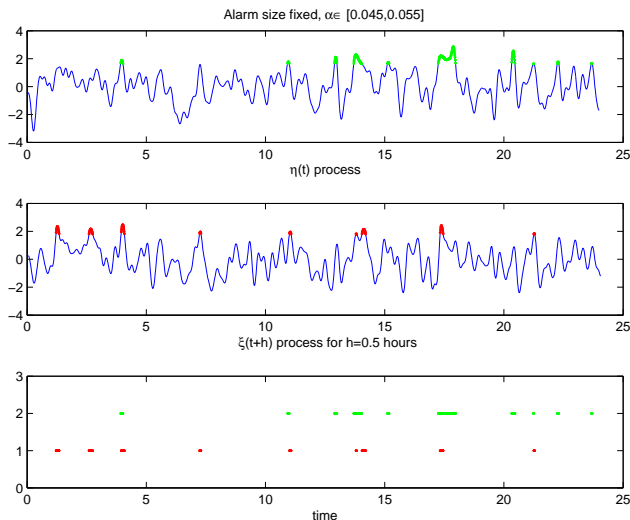


FIGURE 4. *Top*: Simulation of the alarm process  $\eta((-1, 2), t)$ , with green indicating that an alarm is in progress. *Middle*: Simulation of the catastrophe process  $\xi(\mathbf{0}, t - 0.5)$ , with red indicating a catastrophe is occurring. *Bottom*: Green lines indicate when an alarm is in progress and red lines when a catastrophe is occurring.

considered for the alarm process in Case (1) will be considered here, giving six different scenarios.

The cross-covariance functions between the catastrophe process and the two alarm processes and between the time derivative of the catastrophe process and the two alarm processes will obviously interplay to determine the shape of the optimal alarm region, which in this case seems to be elliptical. Again, the region is bounded as the alarm processes can not take on high values with an upcrossing (for the start of a catastrophe) occurring at a later time not far into the future. These cross-covariance functions are similar to those illustrated in Figure 1. Naturally, the scaling and the location will be different for the different pairs.

The optimal alarm regions for different combinations of possible alarm locations were determined in a similar manner to Case (1) and are given in Figure 5. The plotted regions from top left to bottom right correspond to the different combinations as follows:  $((-1, 2), (-0.4, 1))$ ,  $((-1, 2), (0.2, -0.4))$ ,  $((-1, 2), (2.25, -3))$ ,  $((-0.4, 1), (0.2, -0.4))$ ,  $((-0.4, 1), (2.25, -3))$  and  $((0.2, -0.4), (2.25, -3))$ . Again, the relative width seems to reduce as the correlation between the catastrophe process and the corresponding alarm process seems to increase (so the alarm

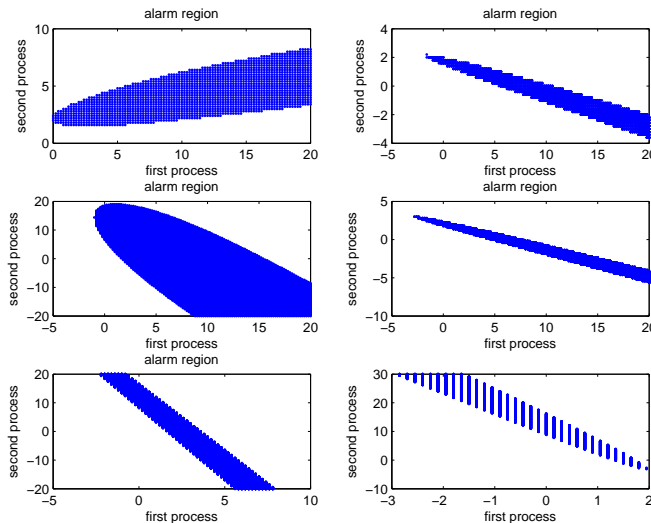


FIGURE 5. Optimal alarm regions for six different pairs of alarm locations.

process located at  $(0.2, -0.4)$  seems to have the narrowest region and that at  $(2.25, -3)$  the widest). In addition, as the alarm size is now “shared” between the two alarm processes, there is, in some sense a narrowing of the alarm “interval” from Case (1) to Case (2) for the individual alarm processes.

The risk and detection probabilities for a catastrophe occurring at  $\mathbf{s}_{01} = \mathbf{0}$ , and alarms located at  $\mathbf{s}_{11} = (-1, 2)$  and  $\mathbf{s}_{11} = (-0.4, 1)$  and with alarm size  $\alpha \in [0.0425, 0.0575]$  have been computed using 10 day simulations of the alarm and catastrophe processes. These have been plotted in Figure 6 (top and bottom respectively) for warning times between 0 and 3, and time step of 0.25.

Again, simulations of the alarm and catastrophe processes were obtained (see Figure 7) for illustrative purposes. The locations for the alarm processes are  $(-1, 2)$  and  $(-0.4, 1)$ , with the catastrophe process at  $\mathbf{s}_{01} = \mathbf{0}$ . As before, the red sections indicate the times a catastrophe is occurring, while the green sections indicate the alarm times for a possible catastrophe  $h = 0.5$  time units later, using an alarm size of  $\alpha \in [0.0425, 0.0575]$ .

**Case (3)** For this case, the reverse setting to Case (2) is considered. Hence, there are two locations for the catastrophe process and a single location for the alarm process. The same four locations as previously for the alarm process are considered. The previous location for the catastrophe process is considered, paired with either  $\mathbf{s}_{02} = (0.4, 0.7)$  or  $\mathbf{s}_{02} = (1.2, 2)$ . For

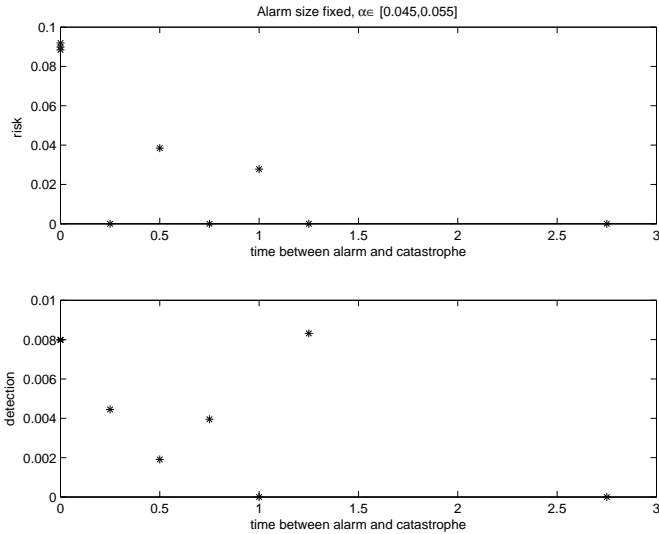


FIGURE 6. Risk probability (*top*) and detection probability (*bottom*) by warning times for catastrophe location  $\mathbf{s}_{01} = \mathbf{0}$ , alarm locations  $\mathbf{s}_{11} = (-1, 2)$  and  $\mathbf{s}_{11} = (-0.4, 1)$ , and alarm size  $\alpha \in [0.0425, 0.0575]$ .

this case, a catastrophe occurs if a catastrophe occurs at either location, with a catastrophe occurring at  $\mathbf{s}_{01} = \mathbf{0}$  if the process exceeds  $u_1 = 2$  and a catastrophe occurring at  $\mathbf{s}_{02}$  if the process exceeds  $u_2 = 1.7$ . Results are presented for both cases, with  $\mathbf{s}_{02} = (0.4, 0.7)$  first.

The optimal alarm regions have been obtained as before and are shown in Figure 8, with the catastrophe locations indicated by an asterisk. As with Case (1), the regions are again bounded intervals. As the alarm process now has to compromise between the two catastrophe processes, while retaining the same alarm size, the intervals, for these locations, have changed by having a smaller lower bound and, consequently, a shorter interval as compared to Case (1).

The risk and detection probabilities have been computed as earlier. These have been plotted in Figure 9 (top and bottom respectively) for warning times between 0 and 3, and time step of 0.25.

For this case, an alarm indicates a potential catastrophe at either of the two catastrophe locations, without indicating at which the catastrophe is likely to occur. In the simulations of the alarm process (top panel) and the catastrophe processes (middle two panels) in Figure 10, a sense of how this works is given. In the bottom panel of Figure 10, the red sections

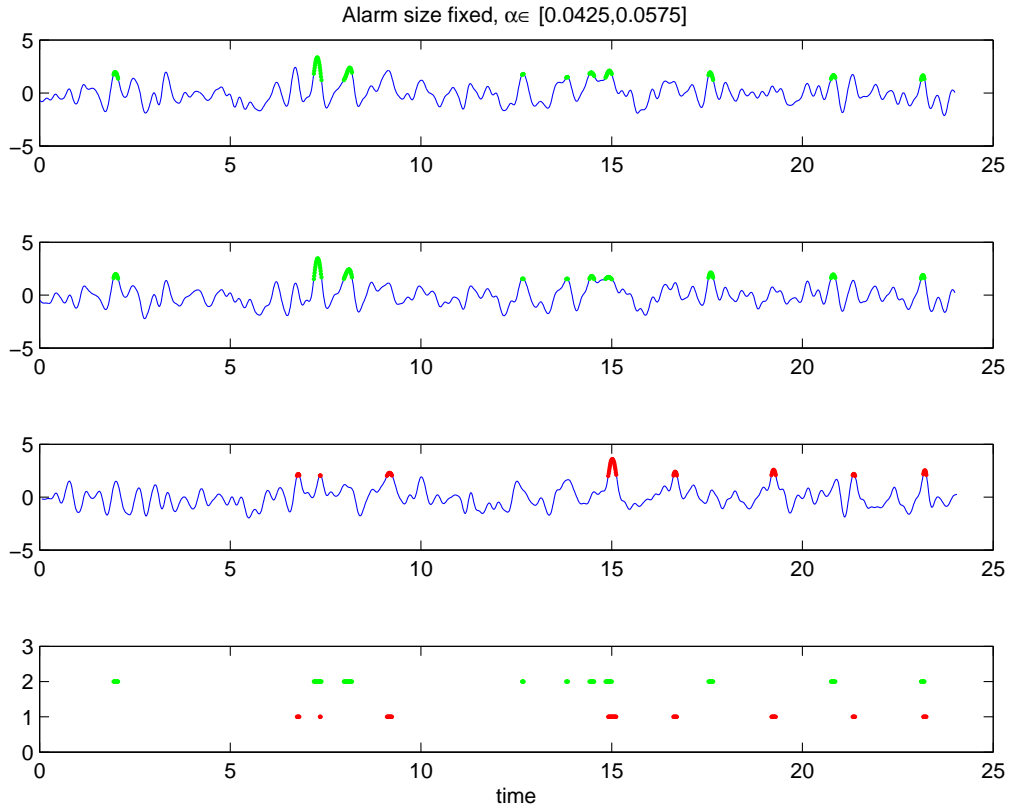


FIGURE 7. *First two panels:* Simulation of alarm processes  $\eta((-1, 2), t)$  and  $\eta((-0.4, 1), t)$ , with green indicating when an alarm is in progress. *Third panel:* Simulation of the catastrophe process  $\xi(\mathbf{0}, t - 0.5)$ , with the red indicating a catastrophe is occurring. *Bottom:* Green lines indicate when an alarm is in progress and red lines when a catastrophe is occurring.

indicate the times at which a catastrophe is occurring, with black indicating those times that this occurs at the first location and with blue the times that this is at the second location. As before green was used to indicate an alarm is in progress, using an alarm size of  $\alpha \in [0.0425, 0.0575]$ .

The above investigation was repeated for  $\mathbf{s}_{02} = (1.2, 2)$ . The optimal alarm regions are given in Figure 11, with the location of the two catastrophe processes indicated by an asterisk. The risk and detection probabilities are given in Figure 12. Finally, simulations of the alarm process and catastrophe processes (as in 10) are given in Figure 13. Although the second catastrophe process is located a little further away from the first location (at  $\mathbf{s}_{01} = \mathbf{0}$ ) for this case, the results have changed little.

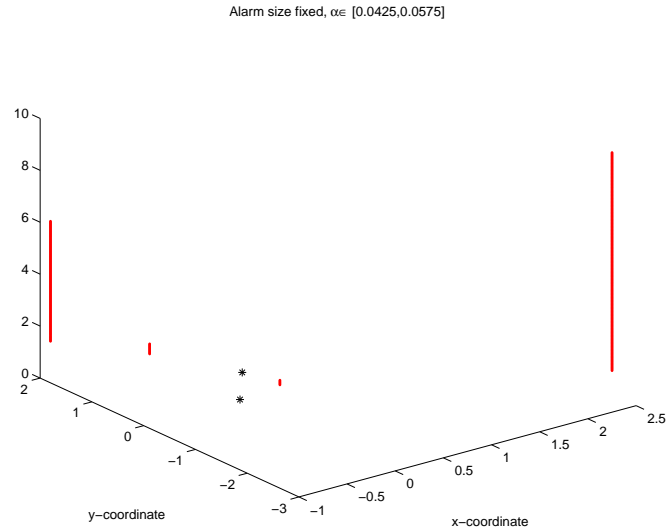


FIGURE 8. Optimal alarm regions for each of the four alarm locations with catastrophe locations at  $\mathbf{s}_{01} = \mathbf{0}$  and  $\mathbf{s}_{02} = (0.4, 0.7)$ .

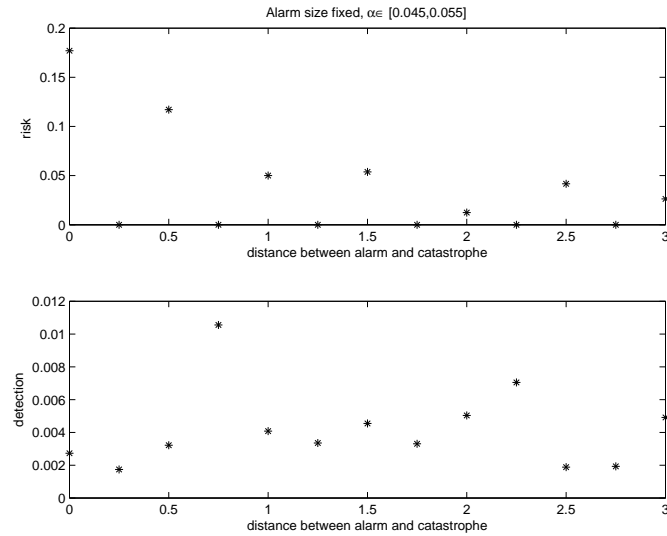


FIGURE 9. Risk probability (*top*) and detection probability (*bottom*) by warning times for catastrophe locations  $\mathbf{s}_{01} = \mathbf{0}$  and  $\mathbf{s}_{02} = (0.4, 0.7)$ , alarm location  $\mathbf{s}_{11} = (-1, 2)$  and alarm size  $\alpha \in [0.0425, 0.0575]$ .

**Case (4)** This case combines the settings in Cases (2) and (3) with the alarm process observed at two locations  $\mathbf{s}_{1i}, i = 1, 2$ , using the same combinations of locations as in the previous cases, and with two locations at which catastrophes are of interest,  $\mathbf{s}_{0i}, i = 1, 2$ , using the same two pairs of locations as in Case (3), with results presented for both. The same

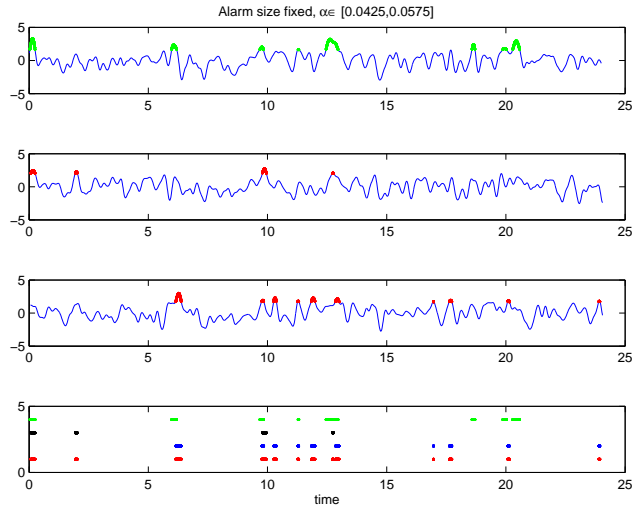


FIGURE 10. *First panel:* Simulation of the alarm process  $\eta((-1, 2), t)$ , with green indicating that an alarm is in progress. *Second and third panel:* Simulation of the catastrophe processes  $\xi(\mathbf{0}, t - 0.5)$  and  $\xi((0.4, 0.7), t - 0.5)$ , with the red indicating a catastrophe is occurring. *Bottom:* Green lines indicate when an alarm is in progress and red lines when a catastrophe is occurring, while black indicates those catastrophes at the first location and blue indicates those catastrophes at the second location.

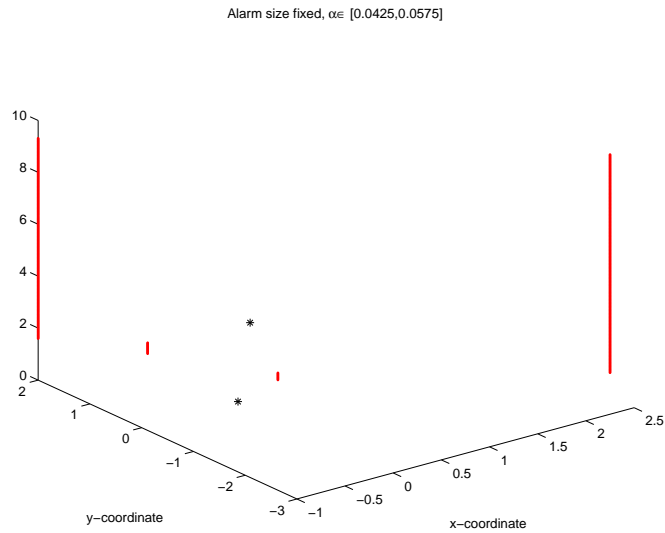


FIGURE 11. Optimal alarm regions for each of the four alarm locations with catastrophe locations at  $\mathbf{s}_{01} = \mathbf{0}$  and  $\mathbf{s}_{02} = ((1.2, 2))$ .

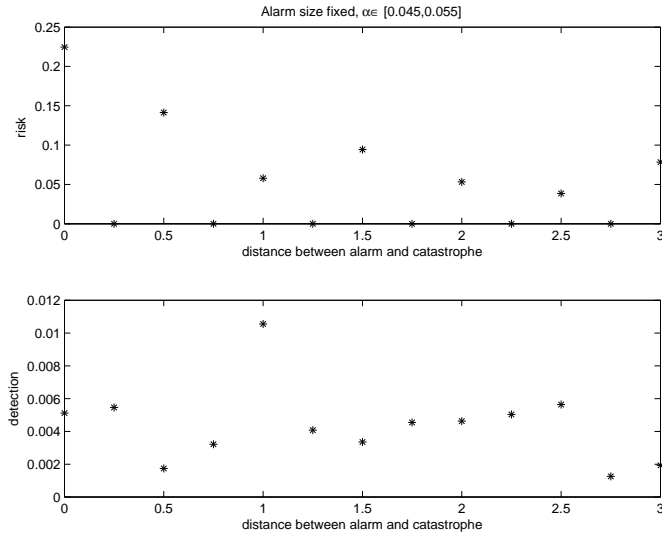


FIGURE 12. Risk probability (*top*) and detection probability (*bottom*) by warning times for catastrophe locations  $\mathbf{s}_{01} = \mathbf{0}$  and  $\mathbf{s}_{02} = (1.2, 2)$ , alarm location  $\mathbf{s}_{11} = (-1, 2)$  and alarm size  $\alpha \in [0.0425, 0.0575]$ .

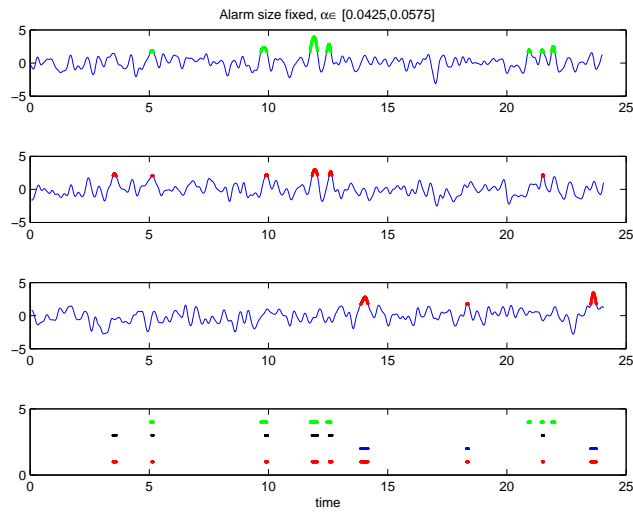


FIGURE 13. *First panel*: Simulation of the alarm process  $\eta((-1, 2), t)$ , with green indicating that an alarm is in progress. *Second and third panel*: Simulation of the catastrophe processes  $\xi(\mathbf{0}, t - 0.5)$  and  $\xi((1.2, 2), t - 0.5)$ , with the red indicating a catastrophe is occurring. *Bottom*: Green lines indicate when an alarm is in progress and red lines when a catastrophe is occurring, while black indicates those catastrophes at the first location and blue indicates those catastrophes at the second location.

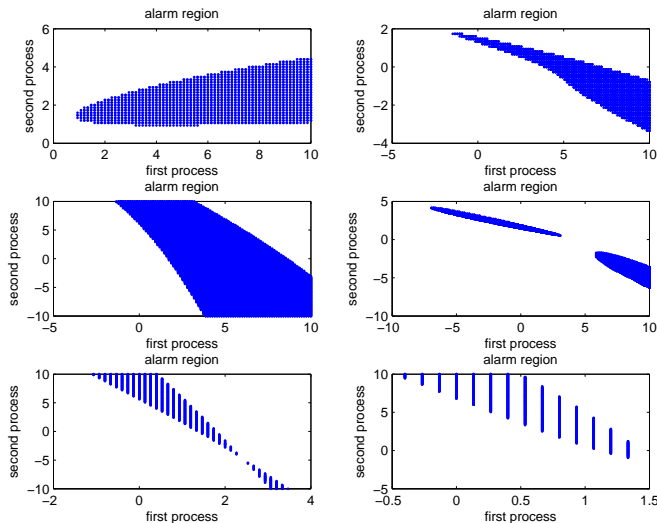


FIGURE 14. Optimal alarm regions for six different combinations of alarm locations and catastrophe locations at  $\mathbf{s}_{01} = \mathbf{0}$  and  $\mathbf{s}_{02} = (0.4, 0.7)$ .

catastrophe setting as in Case (3) is used (with levels  $u_1 = 2$  and  $u_2 = 1.7$ ) and the optimal alarm region was computed using a time lag of  $h = 0.5$  hours and for  $\alpha \in [0.045, 0.055]$ .

The optimal alarm regions for the six combinations of alarm locations have been determined as before and are given in Figure 14 for  $\mathbf{s}_{02} = (0.4, 0.7)$  and in Figure 15 for  $\mathbf{s}_{02} = (1.2, 2)$ , with the location of the two catastrophe processes indicated by an asterisk. Here, the two alarm processes are indicating potential catastrophes at two locations and the optimal alarm region can be more complicated than for the previous cases, with the possibility of consisting of disjoint regions, as seen in both these sets of plots.

The risk and detection probabilities have been computed as earlier. These have been plotted (top and bottom respectively) in Figure 16 for catastrophe locations at  $\mathbf{s}_{01} = \mathbf{0}$  and  $\mathbf{s}_{02} = (0.4, 0.7)$  and in Figure 17 for catastrophe locations at  $\mathbf{s}_{01} = \mathbf{0}$  and  $\mathbf{s}_{02} = (1.2, 2)$ , with alarm locations at  $\mathbf{s}_{11} = (-1, 2)$  and  $\mathbf{s}_{11} = (-0.4, 1)$ , warning times between 0 and 3, and time step of 0.25.

As before, simulations can give some indication of how the two alarm processes give alarms for the two catastrophe processes. These simulations are given in Figure 18 and Figure 19 for  $\mathbf{s}_{01} = \mathbf{0}$  and  $\mathbf{s}_{02} = (0.4, 0.7)$ , and in Figure 20 and Figure 21 for  $\mathbf{s}_{01} = \mathbf{0}$  and  $\mathbf{s}_{02} = (1.2, 2)$ , and for both,  $\mathbf{s}_{11} = (-1, 2)$  and  $\mathbf{s}_{11} = (-0.4, 1)$ .

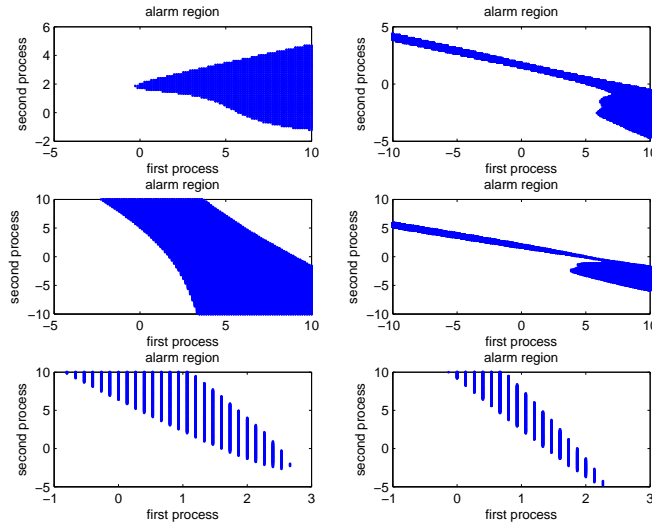


FIGURE 15. Optimal alarm regions for six different combinations of alarm locations and catastrophe locations at  $\mathbf{s}_{01} = \mathbf{0}$  and  $\mathbf{s}_{02} = (1.2, 2)$ .

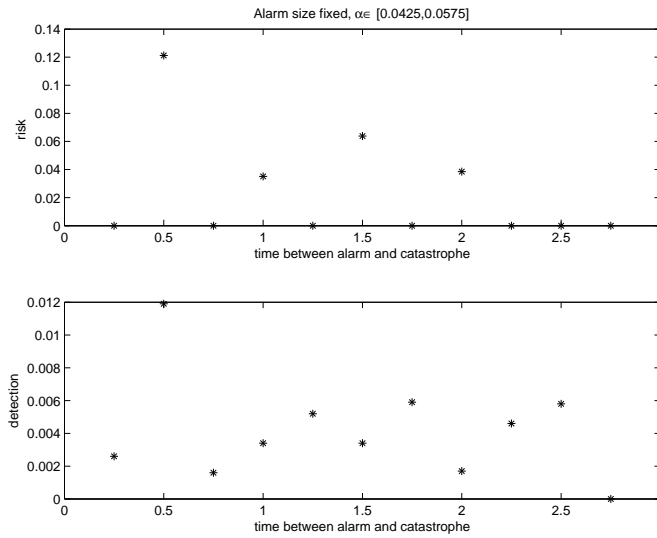


FIGURE 16. Risk probability (*top*) and detection probability (*bottom*) by warning times for catastrophe locations  $\mathbf{s}_{01} = \mathbf{0}$  and  $\mathbf{s}_{02} = (0.4, 0.7)$ , alarm locations  $\mathbf{s}_{11} = (-1, 2)$  and  $\mathbf{s}_{11} = (-0.4, 1)$ , and alarm size  $\alpha \in [0.045, 0.055]$ .

## REFERENCES

- [1] Adler, R. J. and Taylor, J. E.,(2007). *Random Fields and Geometry* Springer Monographs in Mathematics.
- [2] Anderson, T. W.,(1958). *Introduction to Multivariate Statistical Analysis* Wiley, New York.
- [3] Antunes, M., Turkman, K. F. and Amaral Turkman, M.A., (2003). A Bayesian approach to event prediction. *J. Time Ser. Anal.* **24**, No. 6, pp. 631-646.

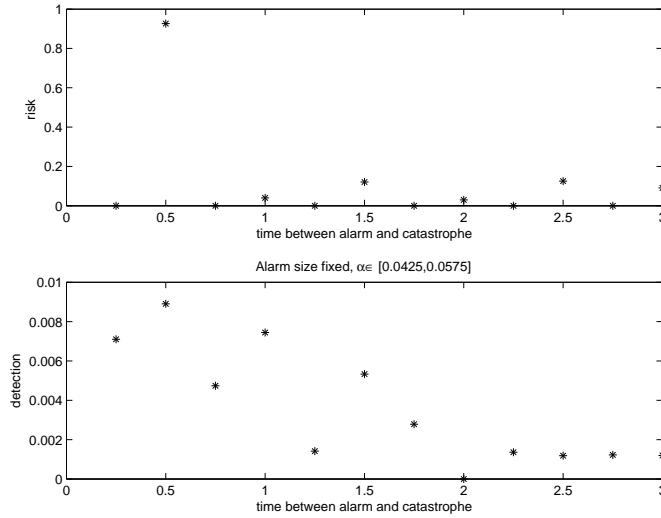


FIGURE 17. Risk probability (*top*) and detection probability (*bottom*) by warning times for catastrophe locations  $\mathbf{s}_{01} = \mathbf{0}$  and  $\mathbf{s}_{02} = (1.2, 2)$ , alarm locations  $\mathbf{s}_{11} = (-1, 2)$  and  $\mathbf{s}_{12} = (-0.4, 1)$ , and alarm size  $\alpha \in [0.045, 0.055]$ .

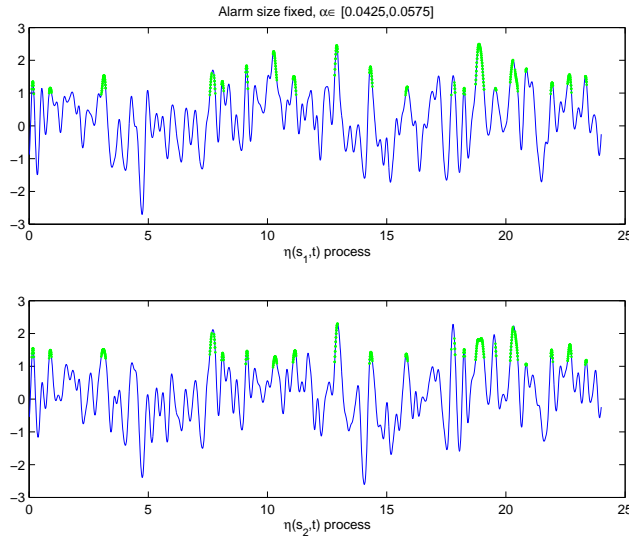


FIGURE 18. Simulation of the alarm processes  $\eta(\mathbf{s}_{1i}, t), i = 1, 2$  for  $\mathbf{s}_{11} = (-1, 2)$  and  $\mathbf{s}_{12} = (-0.4, 1)$ , with green indicating that an alarm is in progress for  $\mathbf{s}_{01} = \mathbf{0}$  and  $\mathbf{s}_{02} = (0.4, 0.7)$ .

[4] Baxevani, A., Podgórski, K., Rychlik, I., (2010). Dynamically evolving Gaussian spatial fields, *Extremes*, **14**, pp. 223-251.  
 [5] Baxevani, A., Borget, C., Rychlik, I., (2008). Spatial Models for the Variability of the Significant Wave Height on the World Oceans. *International Journal of Offshore and Polar Engineering* **18**, pp. 1-7.

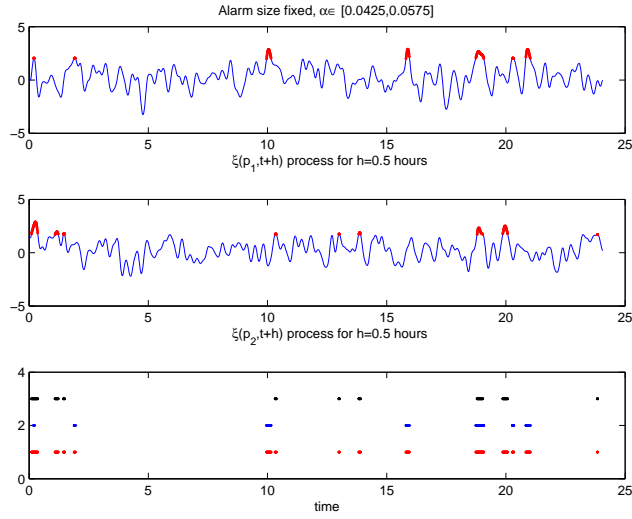


FIGURE 19. *Top two panels:* Simulation of catastrophe processes  $\xi(\mathbf{0}, t - 0.5)$  and  $\xi((0.4, 0.7), t - 0.5)$ , with red indicating a catastrophe is occurring. *Bottom:* Red lines indicate when a catastrophe is occurring, while black indicates those catastrophes at the first location and blue indicates those catastrophes at the second location.

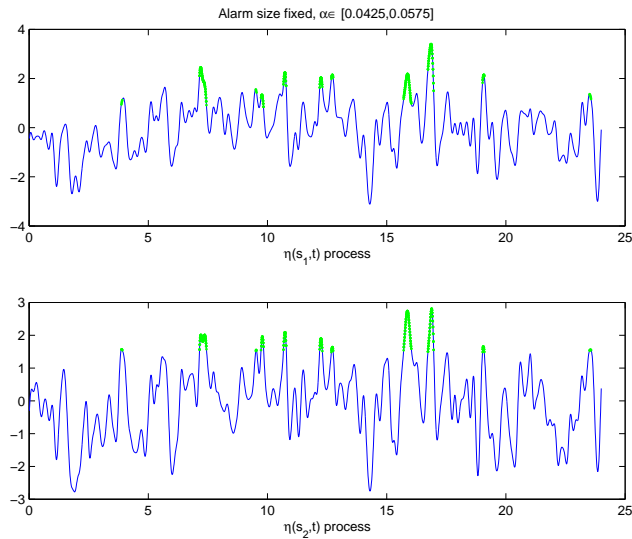


FIGURE 20. Simulation of the alarm processes  $\eta(\mathbf{s}_{1i}, t)$ ,  $i = 1, 2$  for  $\mathbf{s}_{11} = (-1, 2)$  and  $\mathbf{s}_{12} = (-0.4, 1)$ , with green indicating that an alarm is progress for  $\mathbf{s}_{01} = \mathbf{0}$  and  $\mathbf{s}_{02} = (1.2, 2)$ .

- [6] Baxevani, A., Caires, S. Rychlik, I. (2009). Spatio-temporal Statistical Modelling of Significant Wave Height. *Environmetrics*, **20**, pp. 14-31.

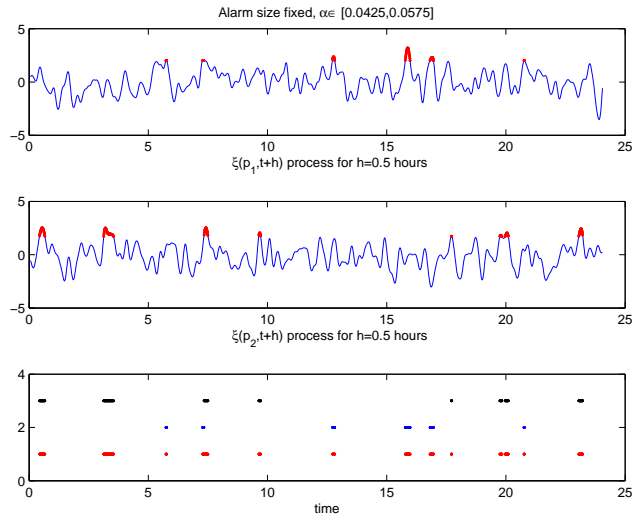


FIGURE 21. *Top two panels:* Simulation of catastrophe processes  $\xi(\mathbf{0}, t - 0.5)$  and  $\xi(1.2, 2, t - 0.5)$ , with red indicating a catastrophe is occurring. *Bottom:* Red lines indicate when a catastrophe is occurring, while black indicates those catastrophes at the first location and blue indicates those catastrophes at the second location.

[7] Baxevani, A., Rychlik, I., and Wilsson, R., (2005). A New Method for Modelling the Space Variability of Significant Wave Height. *Extremes*, **8**, pp. 267–294.

[8] Baxevani, A., Rychlik, I. (2007) Fatigue Life Prediction for a Vessel Sailing the North Atlantic Route, *Probabilistic Engineering Mechanics*, **22**, pp. 159-169.

[9] Borgman, L. E., (1969). Ocean wave Simulation for Engineering Design, *ASCE Jour. Waterw., Port, Coastal and Ocean Engr.*, **95**, pp. 557-583

[10] Buishand, A., de Haan, L. and C. Zhou., (2008). On spatial extremes; with application to a rainfall problem. *Annals of Applied Statistics*, **2**, pp. 624-642.

[11] Costa, C., Scotto, M.G., and Pereira, I. (2010) Optimal alarm systems for FIAParch processes *REVS-TAT*, **8**, pp. 37-55.

[12] De Maré, J., (1980). Optimal prediction of catastrophes with applications to Gaussian processes. *Ann. Probab.*, **8**, pp. 841-850.

[13] Friederichs, P., (2010). Statistical downscaling of extreme precipitation events using extreme value theory. *Extremes*, **13**, pp. 109-132.

[14] Fuentes, A-M., Izzeldin, I. and Kalotychou, E., (2009). On forecasting daily sock volatility: the role of intraday information and market conditions. *Int. J. Forecast.* **25**, pp. 259-281.

- [15] Hopkinson, C.S., Lugo, A.E., Alber, M., Covich, A.P. and Van Bloem, S.J., (2008). Forecasting effects of sea-level rise and windstorms on coastal and inland ecosystems. *Frontiers in Ecology and the Environment*, **6**, pp. 255-263.
- [16] Koop, G. and Tole, L., (2004). Measuring the Health Effects of Air Pollution: To What Extent Can We Really Say that People are Dying from Bad Air? *Journal of Environmental Economics and Management*, **47**, pp. 30-54.
- [17] Lindgren, G., (1980). Model processes in nonlinear prediction with application to detection and alarm. *Ann. Probab.*, **8**, pp. 775-792.
- [18] Lindgren, G., (1985). Optimal Prediction of Level Crossings in Gaussian Processes and Sequences *Ann. Probab.*, **13**, Number 3, pp. 804-824.
- [19] Niedzielski, T. and Kosek, W., (2009). Forecasting sea level anomalies from TOPEX/Poseidon and Jason-1 satellite altimetry. *Journal of Geodesy*, **83**, pp. 469-476.
- [20] Scotto, M.G., Alonso, A.M. and Barbosa, S.M., (2010). Clustering time series of sea levels: extreme value approach. *J. Waterway, Port, Coastal, and Ocean Engrg*, **136**, pp. 215-225.
- [21] Shinozuka, M., (1971). Simulation of multivariate and multi-dimensional random processes. *Journal of the Acoustical Society of America*, **49**, pp. 357-367.
- [22] Smith, R.L., Davis, J.M., Sacks, J., Speckman, P. and Styer, P. (2000). Regression models for air pollution and daily mortality: analysis of data from Birmingham, Alabama, *Environmetrics*, **11**, pp. 719-743.
- [23] Svensson, A., Holst, J., Lindquist, R, and Lindgren, G., (1995). Optimal prediction of catastrophes in autoregressive moving-average processes. *J. Time Ser. Anal.*, **17**, No. 5, pp. 511-531.
- [24] Thomas, L. C., (2000). A survey of credit and behavioural scoring: forecasting financial risk of lending to consumers. *Int. J. Forecast.*, **16**, pp. 149-172.
- [25] Tobias, A. and Scotto, M.G., (2005). Prediction of extreme ozone levels in Barcelona, Spain, *Environ. Monit. Assess.*, **100**, pp. 23-32.
- [26] Turkman, K. F. and Amaral Turkman, M.A., (1989). Optimal Screening Methods. *J. R. Statist. Soc. B*, **51**, No.2, pp. 287-295.
- [27] Weatherford, L.R. and Kimes, S.E., (2003). Forecasting Methods for Hotel Revenue Management: An Evaluation, *International Journal of Forecasting*, **19**, No. 3, pp. 405-419.

## 6. APPENDIX 1

In this section, some results from the theory of multivariate normal densities used in the previous sections are presented. For convenience, the notation of Section 3 will be used. Recall that  $(\boldsymbol{\xi}, \boldsymbol{\eta})$  is assumed to have a zero mean multivariate normal distribution and is

stationary over time, with the components having dimensions  $r$  and  $m$  respectively. Denote the covariance matrix of the vector  $(\boldsymbol{\xi}(h), \dot{\boldsymbol{\xi}}(h), \boldsymbol{\eta}(0))$  by :

$$\begin{pmatrix} \Sigma_{11} & \Sigma_{12} & \Sigma_{13}(h) \\ \Sigma_{21} & \Sigma_{22} & \Sigma_{23}(h) \\ \Sigma_{31}(h) & \Sigma_{32}(h) & \Sigma_{33} \end{pmatrix},$$

where  $\Sigma_{ij}$  denotes the covariance matrix or cross-covariance matrix of the  $(i, j)$ th component vector of  $(\boldsymbol{\xi}(h), \dot{\boldsymbol{\xi}}(h), \boldsymbol{\eta}(0))$ . Below,  $\mathbf{x}$  and  $\mathbf{y}$  denote column vectors of length  $r$  and  $m$  respectively. The following lemma provides the conditional densities used earlier (for derivations of these, see, for example, p.28 of Anderson [2]):

**Lemma 3.** *a)  $\boldsymbol{\xi}(h)$  given  $\boldsymbol{\eta}(0) = \mathbf{y}$  has a multivariate normal distribution with mean*

$$m_{\boldsymbol{\xi}|\boldsymbol{\eta}} = \Sigma_{13}(h)\Sigma_{33}^{-1} \cdot \mathbf{y}$$

*and covariance matrix*

$$\Sigma_{\boldsymbol{\xi}|\boldsymbol{\eta}} = \Sigma_{11} - \Sigma_{13}(h)\Sigma_{33}^{-1}\Sigma_{31}(h).$$

*b)  $\dot{\boldsymbol{\xi}}(h)$  given that  $\boldsymbol{\xi}(h) = \mathbf{x}$  and  $\boldsymbol{\eta}(0) = \mathbf{y}$  has mean*

$$m_{\dot{\boldsymbol{\xi}}|\boldsymbol{\xi}\boldsymbol{\eta}} = (\Sigma_{21} \ \Sigma_{23}) \begin{pmatrix} \Sigma_{11} & \Sigma_{13}(h) \\ \Sigma_{31}(h) & \Sigma_{33} \end{pmatrix}^{-1} \begin{pmatrix} \mathbf{x} \\ \mathbf{y} \end{pmatrix}^T$$

*and variance*

$$\Sigma_{\dot{\boldsymbol{\xi}}|\boldsymbol{\xi}\boldsymbol{\eta}} = \Sigma_{22} - (\Sigma_{21} \ \Sigma_{23}) \begin{pmatrix} \Sigma_{11} & \Sigma_{13}(h) \\ \Sigma_{31}(h) & \Sigma_{33} \end{pmatrix}^{-1} \begin{pmatrix} \Sigma_{12} \\ \Sigma_{32} \end{pmatrix}^T$$

*where  $^T$  denotes transpose.*

## 7. APPENDIX 2

In this section, a method for simulating multi-variate stationary Gaussian processes using their cross-spectral density matrix is presented. Consider a set of  $n$  stationary Gaussian processes  $\xi_i(t)$ , for  $i = 1, \dots, n$ , with mean zero and with a specified cross-spectral density matrix  $S(\omega) = [S_{ij}(\omega)]$ , where  $S_{ij}(\omega)$  is the mean square spectral density of  $\xi_i$  if  $i = j$  and the mean square cross-spectral density of  $\xi_i$  and  $\xi_j$  if  $i \neq j$ . Moreover the spectra have been

standardised so that the variances are equal to one. Following Shinozuka [21], suppose that one can find a matrix  $H(\omega)$  which possesses Fourier transforms and satisfies

$$S(\omega) = H(\omega)\overline{H}(\omega)^T.$$

Then  $\xi_i(t), i = 1, 2, \dots, n$  can be simulated by filtering,

$$(19) \quad \xi_i(t) = \sum_{k=1}^n \int h_{ik}(t - \tau) dB_k(\tau)$$

where  $B_k(\tau)$  are independent Brownian motions and  $h_{ik}(t)$  are the Fourier transforms of  $H_{ik}(\omega)$ .

To find the matrix  $H(\omega)$  in an efficient way, one can assume that  $H(\omega)$  is a lower triangular matrix:

$$H(\omega) = \begin{pmatrix} H_{11}(\omega) & 0 & \dots & 0 \\ H_{21}(\omega) & H_{22} & \dots & 0 \\ \vdots & \vdots & \dots & 0 \\ H_{n1}(\omega) & H_{n2}(\omega) & \dots & H_{nn}(\omega) \end{pmatrix}$$

Hence,

$$(20) \quad \begin{aligned} S_{11}(\omega) &= |H_{11}(\omega)|^2 \\ S_{21}(\omega) &= \overline{S_{12}(\omega)} = H_{21}(\omega)\overline{H_{11}(\omega)} \\ S_{22}(\omega) &= |H_{21}(\omega)|^2 + |H_{22}(\omega)|^2 \end{aligned}$$

and so on. These equations can be sequentially solved for  $H_{ik}(\omega)$ :

$$(21) \quad \begin{aligned} H_{11}(\omega) &= S_{11}(\omega)^{1/2} \\ H_{21}(\omega) &= \frac{S_{21}(\omega)}{S_{11}(\omega)^{1/2}} \\ H_{22}(\omega) &= (S_{22}(\omega) - |H_{21}(\omega)|^2)^{1/2} \end{aligned}$$

and so on.

After solving for the  $H_{ik}(\omega)$ 's, their Fourier transforms are taken to obtain the  $h_{ik}(t)$ 's, which can then be used together with (19) to simulate the processes.

7.1. **Special cases.** At a fixed spatial location  $\mathbf{s}$ , the Gaussian covariance function given in (18) becomes a function of time only. This covariance function is the Fourier transform of the spectrum

$$(22) \quad S(\omega) = \frac{\lambda_0}{\sqrt{2\pi\lambda_{002}/\lambda_0}} \exp\left[-\frac{\omega^2}{2\lambda_{002}/\lambda_0}\right].$$

As well, the cross-covariance function for two processes over time for fixed spatial locations, which differ by  $\mathbf{s} = (s_1, s_2)$ , has Fourier transform

$$(23) \quad \begin{aligned} S^c(\omega) &= S(\omega) \exp\left(i\omega\left(\frac{s_1\lambda_{101} + s_2\lambda_{011}}{\lambda_{002}}\right)\right) \\ &\times \exp\left(\frac{1}{\lambda_0\lambda_{002}}\left\{s_1^2(\lambda_{101}^2 - \lambda_{200}\lambda_{002}) + s_2^2(\lambda_{011}^2 - \lambda_{020}\lambda_{002})\right.\right. \\ &\left.\left.+ 2s_1s_2(\lambda_{101}\lambda_{011} - \lambda_{110}\lambda_{002})\right\}\right). \end{aligned}$$

DEPARTMENT OF MATHEMATICAL SCIENCES, GOTHENBURG UNIVERSITY, CHALMERS UNIVERSITY OF TECHNOLOGY, SE-41296, GOTHENBURG, SWEDEN

*E-mail address:* `anastass@chalmers.se`

SCHOOL OF MATHEMATICS AND PHYSICS, THE UNIVERSITY OF QUEENSLAND, QLD, AUSTRALIA

*E-mail address:* `richard.wilson@uq.edu.au`

DEPARTMENT OF MATHEMATICS, UNIVERSITY OF AVEIRO, PORTUGAL

*E-mail address:* `mscotto@ua.pt`